

Top-Quark Forward-Backward Asymmetry in Randall-Sundrum Models Beyond the Leading Order

M. BAUER, F. GOERTZ, U. HAISCH, T. PFOH AND S. WESTHOFF

*Institut für Physik (THEP), Johannes Gutenberg-Universität
D-55099 Mainz, Germany*

Abstract

We calculate the $t\bar{t}$ forward-backward asymmetry, A_{FB}^t , in Randall-Sundrum (RS) models taking into account the dominant next-to-leading order (NLO) corrections in QCD. At Born level we include the exchange of Kaluza-Klein (KK) gluons and photons, the Z boson and its KK excitations, as well as the Higgs boson, whereas beyond the leading order (LO) we consider the interference of tree-level KK-gluon exchange with one-loop QCD box diagrams and the corresponding bremsstrahlungs corrections. We find that the strong suppression of LO effects, that arises due to the elementary nature and the mostly vector-like couplings of light quarks, is lifted at NLO after paying the price of an additional factor of $\alpha_s/(4\pi)$. In spite of this enhancement, the resulting RS corrections in A_{FB}^t remain marginal, leaving the predicted asymmetry SM-like. As our arguments are solely based on the smallness of the axial-vector couplings of light quarks to the strong sector, our findings are model-independent and apply to many scenarios of new physics that address the flavor problem via geometrical sequestering.

Contents

1	Introduction	1
2	Top-Antitop Production in the SM	4
3	Cross Section and Asymmetry in RS Models	6
3.1	Calculation of LO Effects	7
3.2	Calculation of NLO Effects	12
4	Numerical Analysis	14
5	Conclusions and Outlook	19
A	Higgs-Boson Phase-Space Factors	21
B	Wilson Coefficients in the ZMA	21
C	RG Evolution of the Wilson Coefficients	23
D	Parameter Points	23

1 Introduction

The top quark is the heaviest particle in the Standard Model (SM) of particle physics. Its large mass suggests that it might be deeply connected to the mechanism driving electroweak symmetry breaking. Detailed experimental studies of the top-quark properties are thus likely to play a key role in unravelling the origin of mass, making top-quark observables one of the cornerstones of the Fermilab Tevatron and CERN Large Hadron Collider (LHC) physics programmes.

Up to now, the CDF and DØ experiments at the Tevatron have collected thousands of top-quark pair events, which allowed them to measure the top-quark mass, m_t , and its total inclusive cross section, $\sigma_{t\bar{t}}$, with an accuracy of below 1% [1] and 10% [2, 3], respectively. While these measurements are important in their own right, from the point of view of searches for physics beyond the SM, determinations of kinematic distributions and charge asymmetries in $t\bar{t}$ production are more interesting, since these observables are particularly sensitive to non-standard dynamics. Such searches have been performed at the Tevatron [4, 5, 6], and a result for the $t\bar{t}$ invariant mass spectrum, $d\sigma_{t\bar{t}}/dM_{t\bar{t}}$, has been recently obtained from data collected at CDF [7, 8]. The forward-backward asymmetry, A_{FB}^t , has also been measured [9, 10, 11, 12, 13] and constantly found to be larger than expected. In the laboratory ($p\bar{p}$) frame the most recent CDF result reads

$$(A_{\text{FB}}^t)_{\text{exp}}^{p\bar{p}} = (15.0 \pm 5.0_{\text{stat.}} \pm 2.4_{\text{syst.}}) \%, \quad (1)$$

where the quoted uncertainties are of statistical and systematical origin, respectively.¹

At leading order (LO) in QCD, the charge-asymmetric cross section is zero within the SM. Starting from $\mathcal{O}(\alpha_s^3)$ or next-to-leading order (NLO) onward, the quantity A_{FB}^t receives non-vanishing contributions. These arise from the interference of tree-level gluon exchange with one-loop QCD box diagrams and the interference of initial- and final-state radiation. Including NLO as well as electroweak corrections [15, 16], the SM prediction in the $p\bar{p}$ frame for the inclusive asymmetry is [17]

$$(A_{\text{FB}}^t)_{\text{SM}}^{p\bar{p}} = (5.1 \pm 0.6) \%, \quad (2)$$

where the total error includes the individual uncertainties due to different choices of the parton distribution functions (PDFs), the factorization and renormalization scales, and a variation of m_t within its experimental error. Recent theoretical determinations of $(A_{\text{FB}}^t)_{\text{SM}}$, that include the resummation of logarithmically enhanced threshold effects at NLO [18] and next-to-next-to-leading order (NNLO) [19], are in substantial agreement with the latter number. These results together with general theoretical arguments [20] suggest that the value (2) is robust with respect to higher-order QCD corrections, making it a firm SM prediction.

Although the discrepancy between the experimental (1) and the theoretical (2) value of A_{FB}^t is not significant given the sizable statistical error,² the persistently large values of the observed asymmetry have triggered a lot of activity in the theory community [21, 22, 23, 24, 25, 26, 27, 28, 29, 30, 31, 32, 33, 34]. Many scenarios beyond the SM impact A_{FB}^t already at LO by tree-level exchange of new heavy particles with axial-vector couplings to fermions. However, it turns out to be difficult in general to explain the large central experimental value, since any viable model must simultaneously avoid giving rise to unacceptably large deviations in $\sigma_{t\bar{t}}$ and/or $d\sigma_{t\bar{t}}/dM_{t\bar{t}}$, which both show no evidence of non-SM physics. The first class of proposed models envisions new physics in the t channel (or u channel) with large flavor-violating couplings induced either by vector-boson exchange, namely W' [24, 31, 32] and Z' bosons [23, 29, 30, 31, 32, 33], or by exchange of color singlet, triplet, or sextet scalars [26, 27, 28, 29, 30, 32]. On general grounds, it is not easy to imagine how the necessary flavor-changing couplings can be generated naturally without invoking *ad hoc* assumptions. A second class of models involves s -channel tree-level exchange of new vector states [21, 22, 25, 29, 30, 32, 34], preferably color octets to maximize their interference with QCD, that exhibit sizable axial-vector couplings to both the light quarks, g_A^q , and the top quark, g_A^t . In order to achieve a positive shift in A_{FB}^t the new vectors have to couple to the first and the third generation of quarks with opposite axial-vector couplings [35], implying $g_A^q g_A^t < 0$. Examples of theories that were found to lead to a positive shift in the charge asymmetry are scenarios with a warped extra dimension [21] and flavor non-universal chiral color models [25, 34], both featuring heavy exotic partners of the SM gluon.

The purpose of this article is to show that, in the wide class of scenarios beyond the SM that are dominated by virtual exchange of vector bosons in the s channel, the NLO corrections

¹Very recently DØ reported a measurement of $(A_{\text{FB}}^t)_{\text{exp}}^{\text{obs.}} = (8 \pm 4_{\text{stat.}} \pm 1_{\text{syst.}})\%$ for $t\bar{t}$ events that satisfy the experimental acceptance cuts [14]. The corresponding SM prediction reads $(A_{\text{FB}}^t)_{\text{SM}}^{\text{obs.}} = (1_{-1}^{+2})\%$ and is similarly below the observed value.

²With respect to the previously published CDF result [12], the updated measurement (1) is in better agreement with the SM prediction. The former 2σ discrepancy is now a 1.7σ deviation.

to A_{FB}^t can exceed the LO corrections if the axial-vector couplings to the light quarks are suppressed.³ We will argue that this observation applies in particular to new-physics scenarios that explain the hierarchical structures observed in the masses and mixing of the SM fermions geometrically (which is in one-to-one correspondence to the Froggatt-Nielsen mechanism [37]). Since this way of generating fermion hierarchies also entails a suppression of harmful flavor-changing neutral currents (FCNCs), sequestering flavor is likely to be an integral part of any theory where the solution to the fermion puzzle is associated to a new-physics scale low enough to be directly testable at the LHC. While our considerations are for most of the part general, we find it instructive to elucidate them by working out in detail the relevant LO and NLO corrections to A_{FB}^t that arise in Randall-Sundrum (RS) models [38]. This class of constructions can be regarded as the prototype of non-standard scenarios harnessing the idea of split fermions [39] by locating the left- and right-handed fermions at different places in a warped extra dimension. While the localization pattern gives rise to the necessary axial-vector couplings $g_A^{q,t}$ of Kaluza-Klein (KK) gluons to the SM quarks, the couplings g_A^q turn out to be doubly suppressed: first, because the light quarks reside in the ultraviolet (UV) and, second, because their wave functions of different chiralities are localized nearby in the fifth dimension. The light-quark vector couplings g_V^q do not suffer from the latter type of suppression. In contrast, the top-quark axial-vector and vector couplings, $g_{A,V}^t$, can be sizable due to the large overlap of the third-generation up-type quark wave functions with the ones of the KK gluons, all of which are peaked in the infrared (IR). Given the strong suppression of $g_A^q g_A^t$ in the RS framework, it is then natural to ask if the effects in A_{FB}^t that depend on the product $g_V^q g_V^t$ of vector couplings are phenomenologically more important, despite the fact that this combination enters the prediction for the charge asymmetry first at the one-loop level. This question can only be answered by studying the interplay of new-physics contributions to $t\bar{t}$ production at LO and NLO in detail, and this is exactly what we will do in the following.

This article is organized as follows. After reviewing in Section 2 the kinematics and the structure of the various $t\bar{t}$ observables in the SM, we present in Section 3 the calculation of the RS corrections to the total cross section $\sigma_{t\bar{t}}$ and the forward-backward asymmetry A_{FB}^t . At LO we compute the tree-level exchange of KK gluons and photons, the Z boson and its KK resonances, as well as the Higgs boson, while at NLO we take into account the interference of the dominant tree-level KK-gluon exchange with the one-loop QCD box graphs supplemented by real gluon emission. In order to keep our discussion as general as possible, we perform the calculation in an effective-field theory (EFT) obtained after integrating out the heavy KK states. As a result, our analytic formulas are applicable to a wide class of scenarios with non-standard dynamics above the electroweak scale. We then discuss the structure of the LO and NLO corrections that arise from the exchange of KK gluons in the s channel. As anticipated, we find that, due to the strong suppression of the axial-vector couplings of light quarks, the $\mathcal{O}(\alpha_s^3)$ corrections to A_{FB}^t typically dominate over the $\mathcal{O}(\alpha_s^2)$ contributions in warped models. Our detailed numerical analysis of Section 4 confirms this general finding, but also shows that RS effects are too small to explain the anomalously large value of the $t\bar{t}$ charge asymmetry measured at the Tevatron. We conclude in Section 5. In a series of appendices

³The importance of NLO corrections has been briefly mentioned in [36], which discusses the charge asymmetry in the exclusive channel $p\bar{p} \rightarrow t\bar{t}X$.

we collect details on the phase-space factors appearing in the Higgs-boson contribution, give the analytic expressions for the relevant Wilson coefficients, present compact formulas for the renormalization group (RG) evolution of the relevant Wilson coefficients, and detail the parameter points used in our numerical analysis.

2 Top-Antitop Production in the SM

At the Tevatron $t\bar{t}$ pairs are produced in collisions of protons and antiprotons, $p\bar{p} \rightarrow t\bar{t}X$. Within the SM the hadronic process receives partonic Born-level contributions from quark-antiquark annihilation and gluon fusion

$$\begin{aligned} q(p_1) + \bar{q}(p_2) &\rightarrow t(p_3) + \bar{t}(p_4), \\ g(p_1) + g(p_2) &\rightarrow t(p_3) + \bar{t}(p_4), \end{aligned} \quad (3)$$

where the four-momenta $p_{1,2}$ of the initial state partons can be expressed as the fractions $x_{1,2}$ of the four-momenta $P_{1,2}$ of the colliding hadrons, $p_{1,2} = x_{1,2}P_{1,2}$, and $s = (P_1 + P_2)^2$ denotes the hadronic center-of-mass (CM) energy squared. The partonic cross section is a function of the kinematic invariants

$$\hat{s} = (p_1 + p_2)^2, \quad t_1 = (p_1 - p_3)^2 - m_t^2, \quad u_1 = (p_2 - p_3)^2 - m_t^2, \quad (4)$$

and momentum conservation at Born level implies that $\hat{s} + t_1 + u_1 = 0$.

Since we will be interested in the differential cross section with respect to the invariant mass $M_{t\bar{t}} = \sqrt{(p_3 + p_4)^2}$ of the $t\bar{t}$ pair and the angle θ between \vec{p}_1 and \vec{p}_3 in the partonic CM frame, we express t_1 and u_1 in terms of θ and the top-quark velocity β ,

$$t_1 = -\frac{\hat{s}}{2}(1 - \beta \cos \theta), \quad u_1 = -\frac{\hat{s}}{2}(1 + \beta \cos \theta), \quad \beta = \sqrt{1 - \rho}, \quad \rho = \frac{4m_t^2}{\hat{s}}. \quad (5)$$

The hadronic differential cross section may then be written as

$$\frac{d\sigma^{p\bar{p} \rightarrow t\bar{t}X}}{d \cos \theta} = \frac{\alpha_s}{m_t^2} \sum_{i,j} \int_{4m_t^2}^s \frac{d\hat{s}}{s} \mathbb{f}_{ij}(\hat{s}/s, \mu_f) K_{ij} \left(\frac{4m_t^2}{\hat{s}}, \cos \theta, \mu_f \right), \quad (6)$$

where μ_f denotes the factorization scale and we have introduced the parton luminosity functions

$$\mathbb{f}_{ij}(y, \mu_f) = \int_y^1 \frac{dx}{x} f_{i/p}(x, \mu_f) f_{j/\bar{p}}(y/x, \mu_f). \quad (7)$$

The luminosities for $ij = q\bar{q}, \bar{q}q$ are understood to be summed over all species of light quarks, and the functions $f_{i/p}(x, \mu_f)$ ($f_{i/\bar{p}}(x, \mu_f)$) are the universal non-perturbative PDFs, which describe the probability of finding the parton i in the proton (antiproton) with longitudinal momentum fraction x . The hard-scattering kernels $K_{ij}(\rho, \cos \theta, \mu_f)$ are related to the partonic cross sections and have a perturbative expansion in α_s of the form

$$K_{ij}(\rho, \cos \theta, \mu_f) = \sum_{n=0}^{\infty} \left(\frac{\alpha_s}{4\pi} \right)^n K_{ij}^{(n)}(\rho, \cos \theta, \mu_f). \quad (8)$$

In the SM only the hard-scattering kernels with $ij = q\bar{q}, \bar{q}q, gg$ are non-zero at LO in α_s . By calculating the amplitudes corresponding to s -channel gluon exchange one finds

$$K_{q\bar{q}}^{(0)} = \alpha_s \frac{\pi\beta\rho}{8} \frac{C_F}{N_c} \left(\frac{t_1^2 + u_1^2}{\hat{s}^2} + \frac{2m_t^2}{\hat{s}} \right), \quad (9)$$

$$K_{gg}^{(0)} = \alpha_s \frac{\pi\beta\rho}{8(N_c^2 - 1)} \left(C_F \frac{\hat{s}^2}{t_1 u_1} - N_c \right) \left[\frac{t_1^2 + u_1^2}{\hat{s}^2} + \frac{4m_t^2}{\hat{s}} - \frac{4m_t^4}{t_1 u_1} \right],$$

and the coefficient $K_{q\bar{q}}^{(0)}$ is obtained from $K_{q\bar{q}}^{(0)}$ by replacing $\cos\theta$ with $-\cos\theta$. The factors $N_c = 3$ and $C_F = 4/3$ are the usual color factors of $SU(3)_c$.

In the context of our work it will be convenient to follow [18] and to introduce charge-asymmetric (a) and -symmetric (s) averaged differential cross sections. In the former case, we define

$$\frac{d\sigma_a}{d\cos\theta} \equiv \frac{1}{2} \left[\frac{d\sigma^{p\bar{p} \rightarrow t\bar{t}X}}{d\cos\theta} - \frac{d\sigma^{p\bar{p} \rightarrow \bar{t}tX}}{d\cos\theta} \right], \quad (10)$$

with $d\sigma^{p\bar{p} \rightarrow t\bar{t}X}/d\cos\theta$ given in (6). The corresponding expression for the charge-symmetric averaged differential cross section $d\sigma_s/d\cos\theta$ is simply obtained from the above by changing the minus into a plus sign. The notation indicates that in the process labelled by the superscript $p\bar{p} \rightarrow t\bar{t}X$ ($p\bar{p} \rightarrow \bar{t}tX$) the angle θ corresponds to the scattering angle of the top (antitop) quark in the partonic CM frame. Using (10) one can derive various physical observables in $t\bar{t}$ production. For example, the total hadronic cross section is given by

$$\sigma_{t\bar{t}} = \int_{-1}^1 d\cos\theta \frac{d\sigma_s}{d\cos\theta}. \quad (11)$$

We will mainly be interested in the total $t\bar{t}$ charge asymmetry defined by

$$A_c^t \equiv \frac{\int_0^1 d\cos\theta \frac{d\sigma_a}{d\cos\theta}}{\int_0^1 d\cos\theta \frac{d\sigma_s}{d\cos\theta}}. \quad (12)$$

Since QCD is symmetric under charge conjugation, which implies that

$$\left. \frac{d\sigma^{p\bar{p} \rightarrow \bar{t}tX}}{d\cos\theta} \right|_{\cos\theta=c} = \left. \frac{d\sigma^{p\bar{p} \rightarrow t\bar{t}X}}{d\cos\theta} \right|_{\cos\theta=-c}, \quad (13)$$

for any fixed value c , the charge asymmetry can also be understood as a forward-backward asymmetry

$$A_c^t = A_{\text{FB}}^t \equiv \frac{\int_0^1 d\cos\theta \frac{d\sigma^{p\bar{p} \rightarrow t\bar{t}X}}{d\cos\theta} - \int_{-1}^0 d\cos\theta \frac{d\sigma^{p\bar{p} \rightarrow t\bar{t}X}}{d\cos\theta}}{\int_0^1 d\cos\theta \frac{d\sigma^{p\bar{p} \rightarrow t\bar{t}X}}{d\cos\theta} + \int_{-1}^0 d\cos\theta \frac{d\sigma^{p\bar{p} \rightarrow t\bar{t}X}}{d\cos\theta}} = \frac{\sigma_a}{\sigma_s}. \quad (14)$$

For later convenience we express the asymmetric contribution to the cross section as

$$\sigma_a = \frac{\alpha_s}{m_t^2} \sum_{i,j} \int_{4m_t^2}^s \frac{d\hat{s}}{s} \mathcal{F}_{ij}(\hat{s}/s, \mu_f) A_{ij} \left(\frac{4m_t^2}{\hat{s}} \right). \quad (15)$$

An analogous expression holds in the case of the symmetric contribution σ_s with the hard-scattering charge-asymmetric coefficient $A_{ij}(4m_t^2/\hat{s})$ replaced by its symmetric counterpart $S_{ij}(4m_t^2/\hat{s})$.

In the SM the LO coefficients of the symmetric part read

$$\begin{aligned} S_{q\bar{q}}^{(0)} &= \alpha_s \frac{\pi\beta\rho}{27} (2 + \rho), \\ S_{gg}^{(0)} &= \alpha_s \frac{\pi\beta\rho}{192} \left[\frac{1}{\beta} \ln \left(\frac{1 + \beta}{1 - \beta} \right) (16 + 16\rho + \rho^2) - 28 - 31\rho \right], \end{aligned} \quad (16)$$

while the asymmetric contributions $A_{q\bar{q}}^{(0)}$ and $A_{gg}^{(0)}$ both vanish identically. As we will explain in detail in Section 3.2, at NLO a non-zero coefficient $A_{q\bar{q}}^{(1)}$ is generated in the SM, which leads to a forward-backward asymmetry that is suppressed by $\alpha_s/(4\pi)$ with respect to the symmetric cross section.

3 Cross Section and Asymmetry in RS Models

The RS framework was originally proposed to explain the large hierarchy between the electroweak and the Planck scales via red-shifting in a warped fifth dimension. If the SM fermions and gauge bosons are allowed to propagate in the bulk of the extra dimension [40, 41, 42, 43, 44], the RS model is in addition a promising theory of flavor [39, 42, 44, 45, 46, 47].⁴ Since the fermion zero modes are exponentially localized either in the UV (light SM fermions) or IR (heavy SM fermions), the effective Yukawa couplings resulting from their wave-function overlap with the Higgs boson naturally exhibit exponential hierarchies. In this way one obtains an extra-dimensional realization [49, 50] of the Froggatt-Nielsen mechanism [37], in which the flavor structure is accounted for apart from $\mathcal{O}(1)$ factors. Another important feature that follows from the structure of the overlap integrals is that the effective coupling strength of KK gluons to heavy quarks is enhanced relative to the SM couplings by a factor \sqrt{L} [40, 41] because the involved fields are all localized in the IR. Here $L \equiv \ln(M_{\text{Pl}}/M_W) \approx \ln(10^{16}) \approx 37$ denotes the logarithm of the warp factor, which is fixed by the hierarchy between the electroweak (M_W) and the fundamental Planck (M_{Pl}) scales. Since left- and right-handed fermions are localized at different points in the bulk, the KK-gluon couplings to quarks are in general not purely vector-like, but receive non-vanishing axial-vector components. These couplings generate a charge asymmetry in top-quark pair production at LO, which is associated to quark-antiquark annihilation $q\bar{q} \rightarrow t\bar{t}$ and proceeds through tree-level exchange of KK gluons in the s channel. In the RS model, further corrections to A_{FB}^t arise from the fact that the couplings of KK gluons and photons, the Z boson and its KK excitations, as well as the Higgs boson are flavor

⁴A list of further relevant references can be found in [48].

non-diagonal, leading to the flavor-changing $u\bar{u} \rightarrow t\bar{t}$ transition which affects the t channel.⁵ The corresponding diagrams are shown in Figure 1. On the other hand, the gluon-fusion channel $gg \rightarrow t\bar{t}$ does not receive a correction at Born level, since owing to the orthonormality of gauge-boson wave functions the coupling of two gluons to a KK gluon is zero.

3.1 Calculation of LO Effects

Since the KK scale M_{KK} is at least of the order of a few times the electroweak scale, virtual effects appearing in RS models can be described by means of an effective low-energy theory consisting out of dimension-six operators. In the case at hand, the effective Lagrangian needed to account for the effects of intermediate vector and scalar states reads

$$\mathcal{L}_{\text{eff}} = \sum_{q,u} \sum_{A,B=L,R} \left[C_{q\bar{q},AB}^{(V,8)} Q_{q\bar{q},AB}^{(V,8)} + C_{t\bar{u},AB}^{(V,8)} Q_{t\bar{u},AB}^{(V,8)} + C_{t\bar{u},AB}^{(V,1)} Q_{t\bar{u},AB}^{(V,1)} + C_{t\bar{u},AB}^{(S,1)} Q_{t\bar{u},AB}^{(S,1)} \right], \quad (17)$$

where

$$\begin{aligned} Q_{q\bar{q},AB}^{(V,8)} &= (\bar{q}\gamma_\mu T^a P_A q)(\bar{t}\gamma^\mu T^a P_B t), \\ Q_{t\bar{u},AB}^{(V,8)} &= (\bar{u}\gamma_\mu T^a P_A t)(\bar{t}\gamma^\mu T^a P_B u), \\ Q_{t\bar{u},AB}^{(V,1)} &= (\bar{u}\gamma_\mu P_A t)(\bar{t}\gamma^\mu P_B u), \\ Q_{t\bar{u},AB}^{(S,1)} &= (\bar{u}P_A t)(\bar{t}P_B u), \end{aligned} \quad (18)$$

and the sum over q (u) involves all light (up-type) quark flavors. In addition, $P_{L,R} = (1 \mp \gamma_5)/2$ project onto left- and right-handed chiral quark fields, and T^a are the generators of $SU(3)_c$ normalized such that $\text{Tr}(T^a T^b) = T_F \delta_{ab}$ with $T_F = 1/2$. The superscripts V and S (8 and 1) label vector and scalar (color-octet and -singlet) contributions, respectively.

Using the effective Lagrangian (17) it is straightforward to calculate the interference between the tree-level matrix element describing s -channel SM gluon exchange and the s - and t -channel new-physics contributions arising from the Feynman graphs displayed in Figure 1. In terms of the following combinations of Wilson coefficients

$$C_{ij,\parallel}^{(P,a)} = \text{Re} \left[C_{ij,LL}^{(P,a)} + C_{ij,RR}^{(P,a)} \right], \quad C_{ij,\perp}^{(P,a)} = \text{Re} \left[C_{ij,LR}^{(P,a)} + C_{ij,RL}^{(P,a)} \right], \quad (19)$$

the resulting hard-scattering kernels take the form

$$\begin{aligned} K_{q\bar{q},\text{RS}}^{(0)} &= \frac{\beta\rho}{32} \frac{C_F}{N_c} \left[\frac{t_1^2}{\hat{s}} C_{q\bar{q},\perp}^{(V,8)} + \frac{u_1^2}{\hat{s}} C_{q\bar{q},\parallel}^{(V,8)} + m_t^2 \left(C_{q\bar{q},\parallel}^{(V,8)} + C_{q\bar{q},\perp}^{(V,8)} \right) \right], \\ K_{t\bar{u},\text{RS}}^{(0)} &= \frac{\beta\rho}{32} \frac{C_F}{N_c} \left[\left(\frac{u_1^2}{\hat{s}} + m_t^2 \right) \left(\frac{1}{N_c} C_{t\bar{u},\parallel}^{(V,8)} - 2C_{t\bar{u},\parallel}^{(V,1)} \right) + \left(\frac{t_1^2}{\hat{s}} + m_t^2 \right) C_{t\bar{u},\perp}^{(S,1)} \right]. \end{aligned} \quad (20)$$

Notice that as in the SM the coefficient $K_{q\bar{q},\text{RS}}^{(0)}$ ($K_{t\bar{u},\text{RS}}^{(0)}$) is obtained from $K_{q\bar{q},\text{RS}}^{(0)}$ ($K_{t\bar{u},\text{RS}}^{(0)}$) by simply replacing $\cos\theta$ with $-\cos\theta$.

⁵In principle, also the $d\bar{d} \rightarrow t\bar{t}$ transition receives corrections due to the t -channel exchange of the W boson and its KK partners. We have explicitly verified that these effects are negligibly small for viable values of M_{KK} . Therefore we will ignore them in the following.

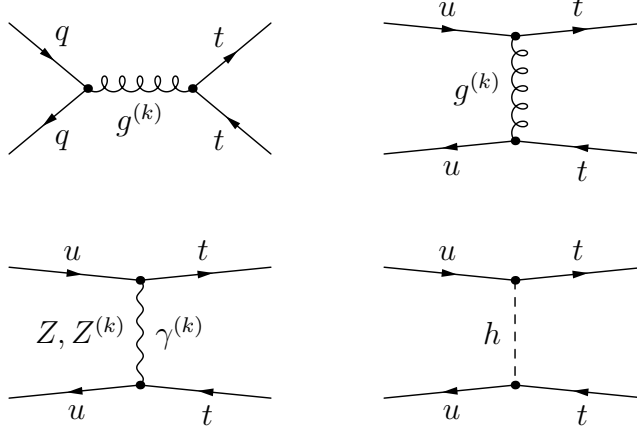


Figure 1: Upper row: Tree-level contributions to the $q\bar{q} \rightarrow t\bar{t}$ (left) and the $u\bar{u} \rightarrow t\bar{t}$ (right) transition arising from s - and t -channel exchange of KK gluons. Lower row: Tree-level contributions to the $u\bar{u} \rightarrow t\bar{t}$ transition arising from t -channel exchange of the Z boson, of KK photons and Z bosons as well as of the Higgs boson. The s -channel (t -channel) amplitudes receive corrections from all light up- and down-type (up-type) quark flavors.

After integrating over $\cos\theta$, one obtains the LO corrections to the symmetric and asymmetric parts of the cross section defined in (15). In the case of the symmetric part we find

$$S_{u\bar{u},\text{RS}}^{(0)} = \frac{\beta\rho}{216} (2 + \rho) \hat{s} \left[C_{u\bar{u},\parallel}^{(V,8)} + C_{u\bar{u},\perp}^{(V,8)} + \frac{1}{3} C_{t\bar{u},\parallel}^{(V,8)} - 2C_{t\bar{u},\parallel}^{(V,1)} \right] + f_S(z) \tilde{C}_{t\bar{u}}^S, \quad (21)$$

$$S_{d\bar{d},\text{RS}}^{(0)} = \frac{\beta\rho}{216} (2 + \rho) \hat{s} \left[C_{d\bar{d},\parallel}^{(V,8)} + C_{d\bar{d},\perp}^{(V,8)} \right],$$

while the asymmetric part in the partonic CM frame takes the form

$$A_{u\bar{u},\text{RS}}^{(0)} = \frac{\beta^2\rho}{144} \hat{s} \left[C_{u\bar{u},\parallel}^{(V,8)} - C_{u\bar{u},\perp}^{(V,8)} + \frac{1}{3} C_{t\bar{u},\parallel}^{(V,8)} - 2C_{t\bar{u},\parallel}^{(V,1)} \right] + f_A(z) \tilde{C}_{t\bar{u}}^S, \quad (22)$$

$$A_{d\bar{d},\text{RS}}^{(0)} = \frac{\beta^2\rho}{144} \hat{s} \left[C_{d\bar{d},\parallel}^{(V,8)} - C_{d\bar{d},\perp}^{(V,8)} \right].$$

Obviously, the coefficients involving down-type quarks do not receive corrections from flavor-changing t -channel transitions. Notice that in (21) the coefficients $C_{q\bar{q},\parallel}^{(V,8)}$ and $C_{q\bar{q},\perp}^{(V,8)}$ enter in the combination $C_{q\bar{q}}^V \equiv (C_{q\bar{q},\parallel}^{(V,8)} + C_{q\bar{q},\perp}^{(V,8)})$, while in (22) they always appear in the form $C_{q\bar{q}}^A \equiv (C_{q\bar{q},\parallel}^{(V,8)} - C_{q\bar{q},\perp}^{(V,8)})$. This feature expresses the fact that the symmetric (asymmetric) LO cross section σ_s (σ_a) measures the product $g_V^q g_V^t$ ($g_A^q g_A^t$) of the vector (axial-vector) parts of the couplings of the KK gluons to light quarks and top quarks. In order to be able to incorporate a light Higgs boson with $m_h \ll M_{\text{KK}}$ into our analysis, we have kept the full

Higgs-boson mass dependence arising from the t -channel propagator.⁶ This dependence is described by the phase-space factors $f_{S,A}(z)$ with $z \equiv m_h^2/m_t^2$. The analytic expressions for $f_{S,A}(z)$ can be found in Appendix A. The new Wilson coefficient $\tilde{C}_{t\bar{u}}^S$ is the dimensionless counterpart of $C_{t\bar{u},\perp}^{(S,1)}$.

The expressions (21) and (22) encode in a model-independent way possible new-physics contributions to $\sigma_{s,a}$ that arise from tree-level exchange of color-octet vectors in the s and t channels, as well as from t -channel corrections due to both new color-singlet vector and scalar states. While this feature should make them useful in general, in the minimal RS model based on an $SU(2)_L \times U(1)_Y$ bulk gauge symmetry, the Wilson coefficients appearing in $S_{ij,RS}^{(0)}$ and $A_{ij,RS}^{(0)}$ take the following specific form. Employing the notation of [48, 49, 51], we find

$$\begin{aligned}
C_{q\bar{q},\parallel}^{(V,8)} &= -\frac{2\pi\alpha_s}{M_{\text{KK}}^2} \left\{ \frac{1}{L} - \sum_{a=Q,q} \left[(\Delta'_a)_{11} + (\Delta'_a)_{33} - 2L (\tilde{\Delta}_a)_{11} \otimes (\tilde{\Delta}_a)_{33} \right] \right\}, \\
C_{q\bar{q},\perp}^{(V,8)} &= -\frac{2\pi\alpha_s}{M_{\text{KK}}^2} \left\{ \frac{1}{L} - \sum_{a=Q,q} \left[(\Delta'_a)_{11} + (\Delta'_a)_{33} \right] + 2L \left[(\tilde{\Delta}_Q)_{11} \otimes (\tilde{\Delta}_Q)_{33} + (\tilde{\Delta}_q)_{11} \otimes (\tilde{\Delta}_q)_{33} \right] \right\}, \\
C_{t\bar{u},\parallel}^{(V,8)} &= -\frac{4\pi\alpha_s}{M_{\text{KK}}^2} L \sum_{a=U,u} \left[(\tilde{\Delta}_a)_{13} \otimes (\tilde{\Delta}_a)_{31} \right], \\
C_{t\bar{u},\parallel}^{(V,1)} &= -\frac{4\pi\alpha_e}{M_{\text{KK}}^2} \frac{L}{s_w^2 c_w^2} \left[(T_3^u - s_w^2 Q_u)^2 (\tilde{\Delta}_U)_{13} \otimes (\tilde{\Delta}_U)_{31} + (s_w^2 Q_u)^2 (\tilde{\Delta}_u)_{13} \otimes (\tilde{\Delta}_u)_{31} \right] \\
&\quad - \frac{4\pi\alpha_e}{M_{\text{KK}}^2} L Q_u^2 \sum_{a=U,u} \left[(\tilde{\Delta}_a)_{13} \otimes (\tilde{\Delta}_a)_{31} \right],
\end{aligned} \tag{23}$$

for $q = u, d$ and $Q = U, D$. Since the coefficient $C_{t\bar{u},\perp}^{(S,1)}$ is formally of $\mathcal{O}(v^4/M_{\text{KK}}^4)$, we do not present its explicit form. Analogous expressions with the index 1 replaced by 2 hold if the quarks in the initial state belong to the second generation. Above, α_s (α_e) is the strong (electromagnetic) coupling constant, s_w (c_w) denotes the sine (cosine) of the weak mixing angle, whereas $T_3^u = 1/2$ and $Q_u = 2/3$ are the isospin and electric charge quantum numbers relevant for up-type quarks. The effective couplings $(\Delta_{Q,q})_{ij}$ comprise the overlap between KK gauge bosons and $SU(2)_L$ doublet (Q) or singlet (q) quarks of generations i and j . Explicit expressions for them can be found in [49]. The coefficients (23) are understood to be evaluated at the KK scale. The inclusion of RG effects, arising from the evolution down to the top-quark mass scale, influences the obtained results only in a minor way. Details on the latter issue can be found in Appendix C. We emphasize that while the expressions for $C_{q\bar{q},\parallel}^{(V,8)}$, $C_{q\bar{q},\perp}^{(V,8)}$, and $C_{t\bar{u},\parallel}^{(V,8)}$ are exact, in the coefficient $C_{t\bar{u},\parallel}^{(V,1)}$ we have only kept terms leading in v^2/M_{KK}^2 . The complete expression for $C_{t\bar{u},\parallel}^{(V,1)}$, including the subleading effects arising from the corrections due to the mixing of fermion zero modes with their KK excitations (that are of $\mathcal{O}(v^4/M_{\text{KK}}^4)$), can be

⁶The observant reader might wonder why we do not introduce form factors for the t -channel contribution arising from the Z -boson as well. The reason is that corrections due to Z -boson exchange turn out to be of $\mathcal{O}(v^4/M_{\text{KK}}^4)$. These effects are hence subleading and we simply ignore them in the following.

easily recovered from [49]. All these corrections will be included in our numerical analysis presented in Section 4.

The expressions for the Wilson coefficients in the extended RS model based on an $SU(2)_R \times SU(2)_L \times U(1)_X \times P_{LR}$ bulk gauge group can be simply obtained from (23) by applying the general formalism developed in [52]. Using this formalism, one finds that the left-handed part of the Z -boson contribution to $C_{t\bar{u},\parallel}^{(V,1)}$ is enhanced by a factor of around 3, while the right-handed contribution is protected by custodial symmetry and thus smaller by a factor of roughly $1/L \approx 1/37$. In contrast, the KK-gluon contributions, encoded in $C_{q\bar{q},\parallel}^{(V,8)}$, $C_{q\bar{q},\perp}^{(V,8)}$, and $C_{t\bar{u},\parallel}^{(V,8)}$, remain unchanged at leading order in $\mathcal{O}(v^2/M_{\text{KK}}^2)$. Taken together these features imply that the predictions for the $t\bar{t}$ observables considered in the course of our work are rather model-independent.

Explicit analytic expressions for the Wilson coefficients (23) in the “zero-mode approximation” (ZMA), which at the technical level corresponds to an expansion of the exact quark wave functions in powers of the ratio of the Higgs vacuum expectation value (VEV) $v \approx 246$ GeV and the KK scale $M_{\text{KK}} = \mathcal{O}(\text{few TeV})$, are given in Appendix B. They depend on the “zero-mode profiles” [42, 44]

$$F(c) = \text{sgn}[\cos(\pi c)] \sqrt{\frac{1+2c}{1-\epsilon^{1+2c}}}, \quad (24)$$

which are themselves functions of the bulk mass parameters $c_{Q_i} \equiv +M_{Q_i}/k$ and $c_{q_i} \equiv -M_{q_i}/k$ that determine the localization of the quark fields in the extra dimension. Here M_{Q_i} and M_{q_i} denote the masses of the five-dimensional (5D) $SU(2)_L$ doublet and singlet fermions, k is the curvature of the 5D anti de-Sitter (AdS₅) space, and $\epsilon \equiv e^{-L} \approx 10^{-16}$.

Restricting ourselves to the corrections proportional to α_s and suppressing relative $\mathcal{O}(1)$ factors as well as numerically subleading terms, one finds from the results given in (B1) that the coefficient functions $S_{ij,\text{RS}}^{(0)}$ and $A_{ij,\text{RS}}^{(0)}$ introduced in (21) and (22) scale in the case of the up quark like

$$S_{u\bar{u},\text{RS}}^{(0)} \sim \frac{4\pi\alpha_s}{M_{\text{KK}}^2} \sum_{A=L,R} F^2(c_{t_A}), \quad (25)$$

$$A_{u\bar{u},\text{RS}}^{(0)} \sim -\frac{4\pi\alpha_s}{M_{\text{KK}}^2} L \left\{ \prod_{q=t,u} [F^2(c_{q_R}) - F^2(c_{q_L})] + \frac{1}{3} \sum_{A=L,R} F^2(c_{t_A}) F^2(c_{u_A}) \right\},$$

where $c_{t_L} \equiv c_{Q_3}$, $c_{t_R} \equiv c_{u_3}$, $c_{u_L} \equiv c_{Q_1}$, and $c_{u_R} \equiv c_{u_1}$.

Under the natural assumptions that the bulk mass parameters of the top and up quarks satisfy $c_{t_A} > -1/2$ and $c_{u_A} < -1/2$,⁷ the relevant $F^2(c_{q_A})$ factors can be approximated by

$$F^2(c_{t_A}) \approx 1 + 2c_{t_A}, \quad F^2(c_{u_A}) \approx (-1 - 2c_{u_A}) e^{L(2c_{u_A}+1)}, \quad (26)$$

with $A = L, R$. The difference of bulk mass parameters for light quarks ($c_{u_L} - c_{u_R}$) is typically small and positive, whereas $(c_{t_L} - c_{t_R})$ can be of $\mathcal{O}(1)$ and is usually negative [48]. Using the

⁷In an anarchic approach to flavor this choice of bulk mass parameters is required to obtain the correct quark masses and mixing angles [45, 46, 47, 48].

above approximations and expanding in powers of $(c_{u_L} - c_{u_R})$, we find

$$\begin{aligned}
S_{u\bar{u},RS}^{(0)} &\sim \frac{4\pi\alpha_s}{M_{\text{KK}}^2} 2(1 + c_{t_L} + c_{t_R}), \\
A_{u\bar{u},RS}^{(0)} &\sim \frac{4\pi\alpha_s}{M_{\text{KK}}^2} 2L e^{L(1+c_{u_L}+c_{u_R})} (1 + c_{u_L} + c_{u_R}) \\
&\times \left\{ \left(2 + \frac{1}{3}\right) L(c_{t_L} - c_{t_R})(c_{u_L} - c_{u_R}) + \frac{1}{3}(1 + c_{t_L} + c_{t_R}) \right\},
\end{aligned} \tag{27}$$

where the symmetric function $S_{u\bar{u},RS}^{(0)}$ is entirely due to s -channel KK-gluon exchange, while the contributions to the asymmetric coefficient $A_{u\bar{u},RS}^{(0)}$ that arise from the s channel (t channel) correspond to the term(s) with coefficient 2 ($1/3$) in the curly bracket.

The relations (27) exhibit a couple of interesting features. We first observe that $S_{u\bar{u},RS}^{(0)}$, which enters the RS prediction for σ_s in (15), is in our approximation independent of the localization of the up-quark fields and strictly positive (as long as $c_{t_A} > -1/2$). This in turn implies an enhancement of the inclusive $t\bar{t}$ production cross section which gets the more pronounced the stronger the right- and left-handed top-quark wave functions are localized in the IR.

In contrast to $S_{u\bar{u},RS}^{(0)}$, both terms in $A_{u\bar{u},RS}^{(0)}$ are exponentially suppressed for UV-localized up quarks, *i.e.*, $c_{u_A} < -1/2$. For typical values of the bulk mass parameters, $c_{t_L} = -0.34$, $c_{t_R} = 0.57$, $c_{u_L} = -0.63$, and $c_{u_R} = -0.68$ [48], one finds numerically that the first term in the curly bracket of (27), which is enhanced by a factor of L but suppressed by the small difference $(c_{u_L} - c_{u_R})$ of bulk mass parameters, is larger in magnitude than the second one by almost a factor of 10. This implies that to first order the charge asymmetry can be described by including only the effects from s -channel KK-gluon exchange. Since generically $(1 + c_{u_L} + c_{u_R})(c_{u_L} - c_{u_R}) < 0$, we furthermore observe that a positive LO contribution to $A_{u\bar{u},RS}^{(0)}$ requires $(c_{t_L} - c_{t_R})$ to be negative, which can be achieved by localizing the right-handed top quark sufficiently far in the IR. To leading powers in hierarchies, one finds using the warped-space Froggatt-Nielsen formulas given in [49] the condition

$$c_{t_R} \gtrsim \frac{m_t}{\sqrt{2}v|Y_t|} - \frac{1}{2}, \tag{28}$$

where the top-quark mass is understood to be normalized at the KK scale and $Y_t \equiv (Y_u)_{33}$ denotes the 33 element of the dimensionless up-type quark Yukawa coupling. Numerically, this means that for $m_t(1 \text{ TeV}) = 144 \text{ GeV}$ and $|Y_t| = 1$ values for c_{t_R} bigger than 0 lead to $A_{u\bar{u},RS}^{(0)} > 0$ and thus to a positive shift in σ_a . Taken together, it turns out that the discussed features of $A_{u\bar{u},RS}^{(0)}$ render the tree-level contribution to the charge asymmetry in the RS framework tiny.⁸ As we will see below in our numerical analysis, the inclusion of electroweak corrections arising from the Born-level exchange of the Z boson, of KK excitations of both the photon and the Z boson as well as of the Higgs boson, do not change this picture qualitatively.

⁸This conclusion can also be drawn from the statements made in [53] concerning the mostly vector-like couplings of light quarks.

3.2 Calculation of NLO Effects

In models with small axial-vector couplings to light quarks and no significant FCNC effects in the t channel, the charge-asymmetric cross section σ_a is suppressed at LO. As we will show in the following, this suppression can be evaded by going to NLO, after paying the price of an additional factor of $\alpha_s/(4\pi)$. In order to understand how the LO suppression is lifted at the loop level, it is useful to recall the way in which the charge asymmetry arises in the SM. Since QCD is a pure vector theory, the lowest-order processes $q\bar{q} \rightarrow t\bar{t}$ and $gg \rightarrow t\bar{t}$, which are of $\mathcal{O}(\alpha_s^2)$ do not contribute to A_{FB}^t . However, starting at $\mathcal{O}(\alpha_s^3)$, quark-antiquark annihilation $q\bar{q} \rightarrow t\bar{t}(g)$, as well as flavor excitation $qg \rightarrow qt\bar{t}$ receive charge-asymmetric contributions [15, 16], while gluon fusion $gg \rightarrow t\bar{t}(g)$, remains symmetric to all orders in perturbation theory. Charge conjugation invariance can be invoked to show that, as far as the virtual corrections to $q\bar{q} \rightarrow t\bar{t}$ are concerned, only the interference between the lowest-order and the QCD box graphs contributes to the asymmetry at NLO. Similarly, for the bremsstrahlungs (or real) contributions, only the interference between the amplitudes that are odd under the exchange of t and \bar{t} furnishes a correction. Since the axial-vector current is even under this exchange, the NLO contribution to the asymmetry arises solely from vector-current contributions. These features imply that at NLO the charge-asymmetric cross section is proportional to the $d_{abc}^2 = (2\text{Tr}(\{T^a, T^b\}T^c))^2$ terms [15, 16] that originate from the interference of both the one-loop box and $t\bar{t}g$ final states with the tree-level quark-antiquark annihilation diagram. The relevant Feynman graphs are obtained from the ones shown in Figure 2 by replacing the operator insertion by an s -channel gluon exchange. The QCD expression for σ_a can be derived from the analogous quantity in the electromagnetic process $e^+e^- \rightarrow \mu^+\mu^-$ [54, 55] by a suitable replacement of the QED coupling and the electromagnetic charges. Explicit formulas for the asymmetric contributions to the $t\bar{t}$ production cross section in QCD are given in [16]. Contributions from flavor excitation are negligibly small at the Tevatron and will not be taken into account in the following.

The main lesson learned from the way the charge asymmetry arises in QCD is that beyond LO vector couplings alone are sufficient to generate non-vanishing values of A_{FB}^t . In the case of the EFT (17) this means that cut diagrams like the ones shown in Figure 2, can give a sizable contribution to the charge asymmetry if the combination $C_{q\bar{q}}^V = (C_{q\bar{q},\parallel}^{(V,8)} + C_{q\bar{q},\perp}^{(V,8)})$ of Wilson coefficients is large enough. In fact, from (21), (22), and (27) it is not difficult to convince oneself that in the case of the RS model NLO corrections to σ_a should dominate over the LO ones, if the condition⁹

$$\frac{\alpha_s}{4\pi} (1 + c_{t_L} + c_{t_R}) \gtrsim L e^{L(1+c_{u_L}+c_{u_R})} \quad (29)$$

is fulfilled. For example, employing $c_{t_L} = -0.34$, $c_{u_L} = -0.63$, and $c_{u_R} = -0.68$, the above formula tells us that for $c_{t_R} = 0.57$ the NLO contributions are bigger than the LO corrections by a factor of roughly 25. This suggests that it might be possible to generate values of A_{FB}^t that can reach the percent level with typical and completely natural choices of parameters. Notice that in contrast to QCD, in the RS framework the Feynman graphs displayed in Figure 2 are not the only sources of charge-asymmetric contributions. Self-energy, vertex, and counterterm

⁹This inequality should be considered only as a crude approximation valid up to a factor of $\mathcal{O}(1)$.

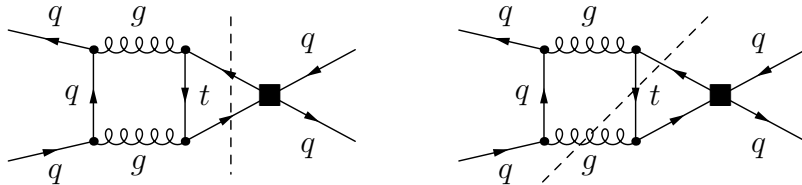


Figure 2: Representative diagrams contributing to the forward-backward asymmetry in $t\bar{t}$ production at NLO. The two-particle (three-particle) cut (represented by a dashed line) corresponds to the interference of $q\bar{q} \rightarrow t\bar{t}$ ($q\bar{q} \rightarrow t\bar{t}g$) with $Q_{q\bar{q},AB}^{(V,8)}$. The insertion of the effective operator is indicated by a black square. The SM contribution is simply obtained by replacing the operator by s -channel gluon exchange.

diagrams will also lead to an asymmetry.¹⁰ However, these corrections are, like the Born-level contribution, all exponentially suppressed by the UV localization of the light-quark fields (and the small axial-vector coupling of the light quarks for what concerns the contributions from the operators $Q_{q\bar{q},AB}^{(V,8)}$). Compared to the tree-level corrections, these contributions are thus suppressed by an additional factor of $\alpha_s/(4\pi)$, so that they can be ignored for all practical purposes.

The above explanations should be motivation enough to perform a calculation of A_{FB}^t in the RS model beyond LO including the graphs depicted in Figure 2. After integrating over $\cos\theta$, we obtain in the partonic CM frame ($q\bar{q} = u\bar{u}, d\bar{d}$)

$$A_{q\bar{q},\text{RS}}^{(1)} = \frac{\hat{s}}{16\pi\alpha_s} C_{q\bar{q}}^V A_{q\bar{q}}^{(1)}, \quad (30)$$

where $A_{q\bar{q}}^{(1)}$ denotes the NLO asymmetric SM coefficient, normalized according to (8). This function can be described through a parametrization which is accurate to the permille level. The result of our fit reads

$$A_{q\bar{q}}^{(1)} = \frac{\alpha_s d_{abc}^2}{16N_c^2} 5.994 \beta\rho \left[1 + 17.948 \beta - 20.391 \beta^2 + 6.291 \beta^3 + 0.253 \ln(1 - \beta) \right], \quad (31)$$

where $N_c = 3$ and $d_{abc}^2 = (N_c^2 - 1)(N_c^2 - 4)/N_c = 40/3$. It has been obtained by integrating the expressions for the charge-asymmetric contributions to the differential $t\bar{t}$ production cross section given in [16] over the relevant phase space.¹¹ In the left panel of Figure 3 we show $A_{q\bar{q}}^{(1)}$ as a function of $\sqrt{\hat{s}}$, employing $m_t = 173.1$ GeV [1] and $\alpha_s(m_t) = 0.126$. We clearly see that the SM distribution $A_{q\bar{q}}^{(1)}$ (solid curve) peaks at around $\sqrt{\hat{s}} \approx 420$ GeV, *i.e.*, relatively close to the $t\bar{t}$ threshold. The NLO RS contribution $A_{q\bar{q},\text{RS}}^{(1)}$ (dashed curve) does not exhibit such a drop-off at large $\sqrt{\hat{s}}$ due to the additional factor of \hat{s} in (30). Since the quark luminosities

¹⁰Box diagrams involving the virtual exchange of one zero-mode and one KK gluon potentially also give a contribution to A_{FB}^t at NLO. We do not include such effects here.

¹¹The numerical integration has been performed using the Vegas Monte Carlo algorithm implemented in the CUBA library [56]

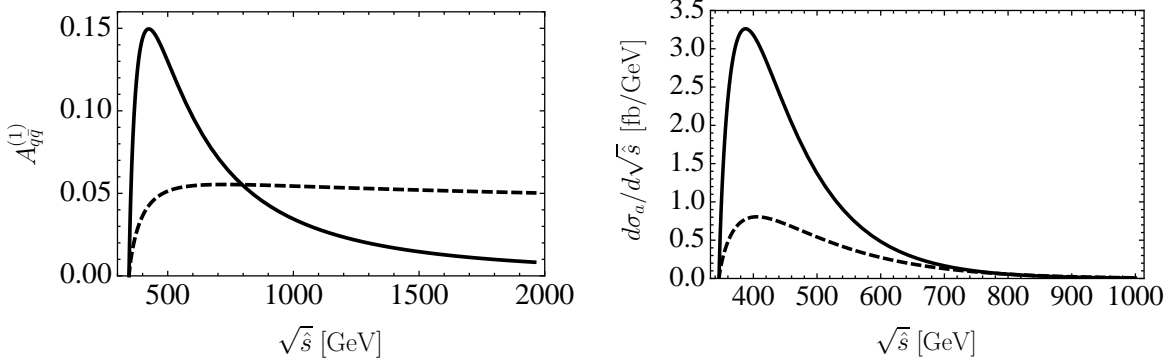


Figure 3: The asymmetric coefficient $A_{q\bar{q}}^{(1)}$ (left panel) and the differential hadronic asymmetry $d\sigma_a/d\sqrt{\hat{s}}$ (right panel) as functions of $\sqrt{\hat{s}}$ in the SM (solid lines) and the RS model (dashed lines). For presentational purposes the shown RS contributions have been obtained using the fictitious value $C_{q\bar{q}}^V = 10/\text{TeV}^2$. See text for further details.

$\mathbb{f}_{ij}(\hat{s}/s, \mu_f)$ fall off strongly with \hat{s} , behaving roughly like $1/\hat{s}^2$, the integrated asymmetry in (15) is saturated well before the upper integration limit s is reached. This can be seen from the right panel in Figure 3, where we multiplied the coefficients $A_{q\bar{q}}^{(1)}$ and $A_{q\bar{q},\text{RS}}^{(1)}$ with the up-quark PDFs $\mathbb{f}_{u\bar{u}}(\hat{s}/s, \mu_f)$.

4 Numerical Analysis

The Wilson coefficients appearing in the effective Lagrangian (17) are constrained by the measurements of the forward-backward asymmetry A_{FB}^t , the total cross section $\sigma_{t\bar{t}}$, and the $t\bar{t}$ invariant mass spectrum $d\sigma_{t\bar{t}}/dM_{t\bar{t}}$. The latest result for A_{FB}^t has already been given in (1) and the most recent Tevatron results ($\sqrt{s} = 1.96 \text{ TeV}$) for the remaining measurements of interest read [2, 7, 8]

$$\begin{aligned}
 (\sigma_{t\bar{t}})_{\text{exp}} &= (7.50 \pm 0.31_{\text{stat.}} \pm 0.34_{\text{syst.}} \pm 0.15_{\text{lumi.}}) \text{ pb}, \\
 \left(\frac{d\sigma_{t\bar{t}}}{dM_{t\bar{t}}} \right)_{\text{exp}}^{M_{t\bar{t}} \in [800, 1400] \text{ GeV}} &= (0.068 \pm 0.032_{\text{stat.}} \pm 0.015_{\text{syst.}} \pm 0.004_{\text{lumi.}}) \frac{\text{fb}}{\text{GeV}}.
 \end{aligned} \tag{32}$$

Here the quoted individual errors are of statistical and systematic origin, and due to the luminosity uncertainty, respectively. Notice that in the case of the $t\bar{t}$ invariant mass spectrum, we have restricted our attention to the last bin of the available CDF measurement, *i.e.*, $M_{t\bar{t}} \in [800, 1400] \text{ GeV}$, which is most sensitive to the presence of new degrees of freedom with masses in the TeV range.

The above results should be compared to the predictions obtained in the SM supplemented by the dimension-six operators (17). Ignoring tiny contributions related to the (anti)strange-, (anti)charm-, and (anti)bottom-quark content of the proton (antiproton), we find in terms of

the dimensionless coefficients $\tilde{C}_{q\bar{q}}^V \equiv 1 \text{ TeV}^2 C_{q\bar{q}}^V$ and $\tilde{C}_{t\bar{u}}^V \equiv 1 \text{ TeV}^2 (1/3 C_{t\bar{u},\parallel}^{(V,8)} - 2C_{t\bar{u},\parallel}^{(V,1)})$ the following expressions

$$\begin{aligned}
(\sigma_{t\bar{t}})_{\text{RS}} &= \left[1 + 0.053 (\tilde{C}_{u\bar{u}}^V + \tilde{C}_{t\bar{u}}^V) - 0.612 \tilde{C}_{t\bar{u}}^S + 0.008 \tilde{C}_{d\bar{d}}^V \right] (6.73_{-0.80}^{+0.52}) \text{ pb}, \\
\left(\frac{d\sigma_{t\bar{t}}}{dM_{t\bar{t}}} \right)_{\text{RS}}^{M_{t\bar{t}} \in [800, 1400] \text{ GeV}} &= \left[1 + 0.33 (\tilde{C}_{u\bar{u}}^V + \tilde{C}_{t\bar{u}}^V) - 0.81 \tilde{C}_{t\bar{u}}^S + 0.02 \tilde{C}_{d\bar{d}}^V \right] (0.061_{-0.006}^{+0.012}) \frac{\text{fb}}{\text{GeV}},
\end{aligned} \tag{33}$$

where all Wilson coefficients are understood to be evaluated at m_t . The numerical factors multiplying $\tilde{C}_{t\bar{u}}^S$ correspond to a Higgs mass of $m_h = 115 \text{ GeV}$, which we will adopt in the following. The RG evolution of the Wilson coefficients from M_{KK} to m_t is achieved with the formulas given in Appendix C. The dependence of $\sigma_{t\bar{t}}$ and $d\sigma_{t\bar{t}}/dM_{t\bar{t}}$ on \tilde{C}_{ij}^P has been obtained by convoluting the kernels (21) with the parton luminosities $\mathcal{f}_{ij}(\hat{s}/s, \mu_f)$ by means of the charge-symmetric analog of formula (15), using MSTW2008LO PDFs [57] with renormalization and factorization scales fixed to the reference point $\mu_r = \mu_f = m_t = 173.1 \text{ GeV}$. The corresponding value of the strong coupling constant is $\alpha_s(M_Z) = 0.139$, which translates into $\alpha_s(m_t) = 0.126$ using one-loop RG running. The total cross section and $t\bar{t}$ invariant mass distribution in the SM have been calculated at NLO [58] with the help of MCFM [59], employing MSTW2008NLO PDFs along with $\alpha_s(M_Z) = 0.120$, corresponding to $\alpha_s(m_t) = 0.109$ at two-loop accuracy. The given total SM errors represent the uncertainty due to the variation $\mu_r = \mu_f \in [m_t/2, 2m_t]$ as well as PDF errors within their 90% confidence level (CL) limits, after combining the two sources of error in quadrature. Notice that within errors our SM prediction for $\sigma_{t\bar{t}}$ is in good agreement with recent theoretical calculations, that include effects of logarithmically enhanced NNLO terms [19, 60, 61, 62, 63].

The forward-backward asymmetry A_{FB}^t as given in (1) is measured in the $p\bar{p}$ frame, while (12), (14), and (15) apply in the partonic CM frame. The transformation from the partonic CM into the $p\bar{p}$ frame corresponds to a mere change of integration boundaries of the scattering angle $\cos\theta$. In order to calculate the asymmetric contribution to the cross section in the $p\bar{p}$ frame, $\sigma_a^{p\bar{p}}$, we employ at Born level,

$$\sigma_a^{p\bar{p}} = \frac{\alpha_s}{m_t^2} \sum_{i,j} \int_{4m_t^2/s}^1 d\tau \int_{\tau}^1 \frac{dx}{x} f_{i/p}(x, \mu_f) f_{j/\bar{p}}(\tau/x, \mu_f) A_{ij}^{p\bar{p}}(x, \tau, \mu_f), \tag{34}$$

where $\tau \equiv \hat{s}/s$ and

$$A_{ij}^{p\bar{p}}(x, \tau, \mu_f) \equiv \int_{c(x,\tau)}^1 d\cos\theta K_{ij}(\rho, \cos\theta, \mu_f) - \int_{-1}^{c(x,\tau)} d\cos\theta K_{ij}(\rho, \cos\theta, \mu_f), \tag{35}$$

with

$$c(x, \tau) \equiv \frac{1}{\beta} \frac{x^2 - \tau}{x^2 + \tau}, \tag{36}$$

and the hard-scattering kernels $K_{ij}(\rho, \cos\theta, \mu_f)$ have been introduced in (8). Beyond LO the phase-space integration is more involved. For convenience we thus give the reduction factors

c_{t_L}	c_{t_R}	$\tilde{C}_{u\bar{u}}^V/\alpha_s$	$\tilde{C}_{u\bar{u}}^A/\alpha_s$	$\tilde{C}_{d\bar{d}}^V/\alpha_s$	$\tilde{C}_{d\bar{d}}^A/\alpha_s$	$\tilde{C}_{t\bar{t}}^V/\alpha_s$	$\tilde{C}_{t\bar{t}}^S$
-0.41	0.09	4.50	$0.71 \cdot 10^{-2}$	0.68	$-1.40 \cdot 10^{-3}$	$-1.35 \cdot 10^{-4}$	$8.2 \cdot 10^{-7}$
-0.47	0.48	4.95	$0.22 \cdot 10^{-2}$	0.27	$-0.03 \cdot 10^{-3}$	$-0.70 \cdot 10^{-4}$	$4.1 \cdot 10^{-7}$
-0.49	0.90	5.31	$1.79 \cdot 10^{-2}$	0.08	$-0.64 \cdot 10^{-3}$	$-2.45 \cdot 10^{-4}$	$122 \cdot 10^{-7}$

Table 1: Results for the Wilson coefficients corresponding to three different parameter points. The numbers shown correspond to the RS model with $SU(2)_L \times U(1)_Y$ bulk gauge symmetry and brane-localized Higgs sector. The coefficients in the first five columns scale as $(1 \text{ TeV}/M_{\text{KK}})^2$ while the one in the last column behaves as $(1 \text{ TeV}/M_{\text{KK}})^4$. Further details are given in the text.

$R \equiv \sigma_a^{p\bar{p}}/\sigma_a$ that are needed to convert the SM as well as the EFT results of the forward-backward asymmetry from the partonic CM to the $p\bar{p}$ frame. In the SM we find $R_{\text{SM}} = 0.64$, while the ratios necessary to calculate the contributions arising from the various effective operators are given by $R_{u\bar{u}}^V = 0.73$, $R_{d\bar{d}}^V = 0.72$, $R_{t\bar{t}}^S = -1.78$, $R_{u\bar{u}}^A = 0.58$, and $R_{d\bar{d}}^A = 0.56$. These numbers correspond to MSTW2008LO PDFs with the renormalization and factorization scales set to the reference point mentioned above.

With all this at hand, we are now in a position to give the forward-backward asymmetry in the laboratory frame. Normalizing the result for $\sigma_a^{p\bar{p}}$ to σ_s calculated at NLO,¹² we find the following expression

$$(A_{\text{FB}}^t)_{\text{RS}}^{p\bar{p}} = \left[\frac{1 + 0.22 (\tilde{C}_{u\bar{u}}^A + \tilde{C}_{t\bar{t}}^V) + 0.72 \tilde{C}_{t\bar{t}}^S + 0.03 \tilde{C}_{d\bar{d}}^A + 0.034 \tilde{C}_{u\bar{u}}^V + 0.005 \tilde{C}_{d\bar{d}}^V}{1 + 0.053 (\tilde{C}_{u\bar{u}}^V + \tilde{C}_{t\bar{t}}^V) - 0.612 \tilde{C}_{t\bar{t}}^S + 0.008 \tilde{C}_{d\bar{d}}^V} \right] (5.6_{-1.0}^{+0.8}) \%, \quad (37)$$

where all coefficient functions should be evaluated at the scale m_t . The central value of our SM prediction has been obtained by integrating the formulas given in [16] over the relevant phase space (see (34) to (36)), weighted with MSTW2008LO PDFs with the unphysical scales fixed to m_t . It is in good agreement with (2) as well as the findings of [18, 19]. Unlike [17], we have chosen not to include electroweak corrections to the forward-backward asymmetry in the central value of (37). Such effects have been found in [17, 64] to enhance the $t\bar{t}$ forward-backward asymmetry by around 9% to 4% depending on whether only mixed electroweak-QCD contributions or also purely electroweak corrections are included. To account for the uncertainty of our SM prediction due to electroweak effects we have added in quadrature an error of 5% to the combined scale and PDF uncertainties.

In order to investigate the importance of the different contributions entering the RS predictions (33) and (37) for the $t\bar{t}$ observables, we have calculated the relevant Wilson coefficients at the KK scale for typical sets of bulk mass parameters and anarchic Yukawa couplings $Y_{u,d}$ (*i.e.*, non-hierarchical matrices with $\mathcal{O}(1)$ complex elements). In Table 1 we present our numerical results for the coefficient functions for three assorted parameter points that reproduce

¹²Using MSTW2008 PDFs and $\mu_r = \mu_f = m_t = 173.1 \text{ GeV}$, we obtain in the SM the symmetric cross sections $(\sigma_s)_{\text{LO}} = 6.66 \text{ pb}$ and $(\sigma_s)_{\text{NLO}} = 6.73 \text{ pb}$ from MCFM. Since these results differ by only 1%, the central value of A_{FB}^t does essentially not depend on whether the LO or the NLO cross section is used to normalize (37).

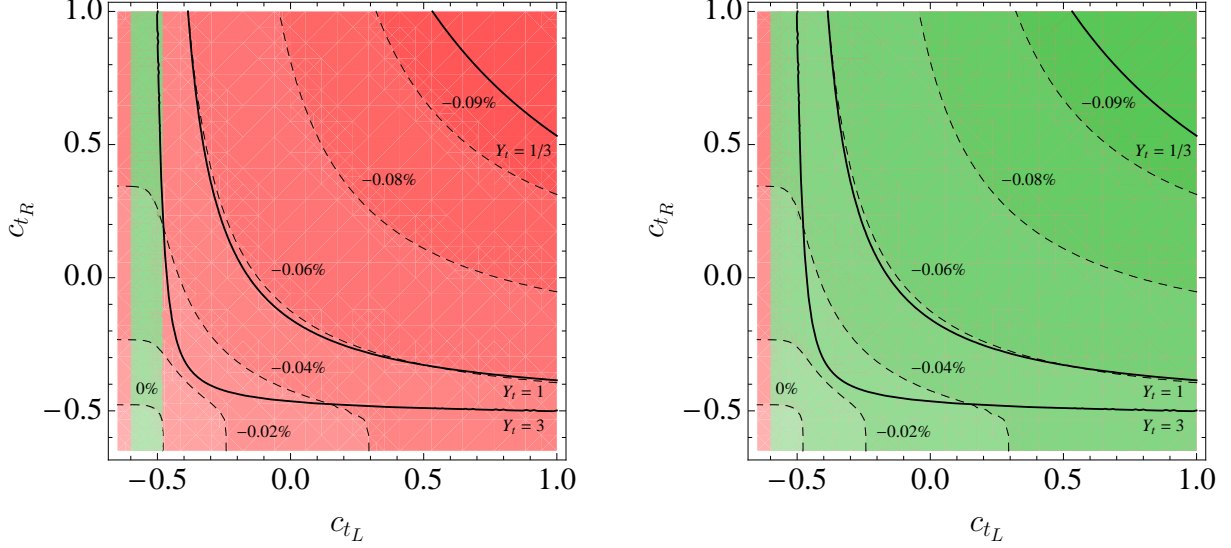


Figure 4: Size of the absolute correction to $(A_{\text{FB}}^t)^{p\bar{p}}_{\text{RS}}$ in the c_{t_L} - c_{t_R} plane for a KK scale of 1 TeV. The solid lines indicate the value of Y_t necessary to reproduce the measured mass of the top quark. In the left (right) panel only the parameter region of the minimal (extended) RS model displayed in green satisfies the constraints imposed by the $Z \rightarrow b\bar{b}$ “pseudo observables”. See text for further details.

the observed quark masses as well as the angles and the CP-violating phase in the quark mixing matrix within errors. To keep the presentation simple, we show in the table only the values of the left- and right-handed top-quark bulk mass parameters c_{t_L} and c_{t_R} . The numerical values for the remaining bulk mass parameters and Yukawa matrices, specifying the three parameter points completely, are relegated to Appendix D. We emphasize that the magnitudes of the shown results are generic predictions in the allowed parameter space and do not reflect a specific choice of model parameters. From the numbers given in the table, we see that the ratios of magnitudes of the Wilson coefficients are given by $|\tilde{C}_{q\bar{q}}^A|/|\tilde{C}_{q\bar{q}}^V| = \mathcal{O}(10^{-3})$, $|\tilde{C}_{t\bar{u}}^V|/|\tilde{C}_{u\bar{u}}^V| = \mathcal{O}(10^{-5})$, and $|\tilde{C}_{t\bar{u}}^S|/|\tilde{C}_{u\bar{u}}^V| = \mathcal{O}(10^{-6})$. For what concerns the size of the corrections due to flavor-changing currents in the t channel (encoded in $\tilde{C}_{t\bar{u}}^V$ and $\tilde{C}_{t\bar{u}}^S$), we mention that in the RS model based on an $SU(2)_L \times U(1)_Y$ bulk gauge group, the ratio of neutral electroweak gauge boson (Higgs-boson) to KK-gluon effects is roughly 1/3 (on average 1/50). In the RS variant with extended $SU(2)_R$ symmetry and custodial protection of the $Zb_L\bar{b}_L$ vertex, one finds a very similar pattern. The quoted numbers imply that the predictions for the $t\bar{t}$ observables considered in our work are fairly model-independent, as they do not depend sensitively on the exact realizations of neither the electroweak gauge, nor the fermionic, nor the Higgs sector.

Focusing on the numerical dominant corrections arising from s -channel KK-gluon exchange, we see from Table 1 that $\tilde{C}_{u\bar{u}}^V$ and $\tilde{C}_{u\bar{u}}^A$ are a factor of a few larger in magnitude than their counterparts involving down quarks. Since the latter coefficients are suppressed in the total cross section (last bin of the $t\bar{t}$ invariant mass spectrum) relative to the coeffi-

icients involving up quarks by the small ratio of quark luminosities $\mathcal{L}_{d\bar{d}}(0.04)/\mathcal{L}_{u\bar{u}}(0.04) \approx 1/5$ ($\mathcal{L}_{d\bar{d}}(0.17)/\mathcal{L}_{u\bar{u}}(0.17) \approx 1/15$), the numerical impact of $\tilde{C}_{d\bar{d}}^V$ in (33) is negligible. In practice, we find that the relevant ratio $(0.008\tilde{C}_{d\bar{d}}^V)/(0.053\tilde{C}_{u\bar{u}}^V)$ ($(0.02\tilde{C}_{d\bar{d}}^V)/(0.33\tilde{C}_{u\bar{u}}^V)$) amounts to less than 2.3% (1.0%) for the considered parameter points. In the following, we will therefore restrict our attention to the coefficients $\tilde{C}_{u\bar{u}}^{V,A}$ that render by far the largest contributions to the $t\bar{t}$ observables in the RS model. From Table 1 we first observe that $\tilde{C}_{u\bar{u}}^V$ grows with increasing $(c_{t_L} + c_{t_R})$, *i.e.*, when the top quark is localized more strongly in the IR (as expected from (27) and (28)). A similar trend in terms of c_{t_R} , though less pronounced, is also visible in the case of $\tilde{C}_{u\bar{u}}^A$. The numbers given in the table furthermore confirm our qualitative findings from Section 3.1 of strongly suppressed axial-vector couplings, $|\tilde{C}_{u\bar{u}}^A|/|\tilde{C}_{u\bar{u}}^V| \ll 1$. Inserting the numerical values of $\tilde{C}_{u\bar{u}}^V$ and $\tilde{C}_{u\bar{u}}^A$ into the numerator of (37), we see that also our third expectation (made in Section 3.2) that in the RS model the NLO contributions to A_{FB}^t arising from $\tilde{C}_{u\bar{u}}^V$ are bigger than the LO corrections stemming from $\tilde{C}_{u\bar{u}}^A$, in fact, holds true. Numerically, we find that the vector-current contributions to the asymmetry are typically larger by about a factor of 100 than the corrections due to the axial-vector current.

While this strong enhancement looks promising at first sight, a closer inspection of (37) shows that in the ratio of the asymmetric and symmetric cross sections the effects of $\tilde{C}_{u\bar{u}}^V$ tend to cancel. Since both $\sigma_a^{p\bar{p}}$ and σ_s are enhanced for $\tilde{C}_{u\bar{u}}^V > 0$, but the dependence of σ_s on $\tilde{C}_{u\bar{u}}^V$ is stronger than the one of $\sigma_a^{p\bar{p}}$, positive values of $\tilde{C}_{u\bar{u}}^V$ will effectively lead to a reduction and not to an enhancement of the $t\bar{t}$ forward-backward asymmetry as envisioned in Section 3.2. Given that $\tilde{C}_{u\bar{u}}^V > 0$ is a robust prediction of the RS framework, following from the composite nature of the top quark, we conclude that the corrections to A_{FB}^t are necessarily negative. This feature is illustrated in Figure 4, which shows the predictions for the absolute RS corrections to the forward-backward asymmetry in the $p\bar{p}$ frame as a function of c_{t_L} and c_{t_R} . The figures have been obtained including only the KK-gluon corrections to $\tilde{C}_{u\bar{u}}^{V,A}$ and employing $M_{\text{KK}} = 1 \text{ TeV}$, $c_{u_L} = c_{d_L} = -0.63$, $c_{u_R} = -0.68$, $c_{d_R} = -0.66$, $c_{c_L} = c_{s_L} = -0.56$, and $c_{c_R} = -0.53$, $c_{s_R} = -0.63$, as well as setting all minors of $Y_{u,d}$ equal (only $Y_t = (Y_u)_{33}$ is allowed to vary in order to reproduce the observed top-quark mass). Both panels show clearly that in the whole c_{t_L} - c_{t_R} plane the corrections to $(A_{\text{FB}}^t)_{\text{RS}}^{p\bar{p}}$ interfere destructively with the SM. However, even for an optimistic value of $M_{\text{KK}} = 1 \text{ TeV}$, corresponding to a mass of the lightest KK gluon of around 2.5 TeV, we find that after imposing the $Z \rightarrow b\bar{b}$ constraints¹³ the maximal attainable effects amount to not even -0.05% (-0.10%) in the minimal (extended) RS model based on an $SU(2)_L \times U(1)_Y$ ($SU(2)_R \times SU(2)_L \times U(1)_X \times P_{LR}$) bulk gauge group.¹⁴ The parameter regions compatible with the $Z \rightarrow b\bar{b}$ data are colored green in Figure 4. While this constraint is very stringent in the minimal model, restricting the allowed parameter space to a thin stripe with $c_{t_L} \in [-0.60, -0.49]$, it does not pose a tight bound in the case of the extended scenario allowing for $c_{t_L} \in [-0.60, 1]$. Since the KK-gluon corrections decouple as $1/M_{\text{KK}}^2$, employing $M_{\text{KK}} = 2 \text{ TeV}$ instead of 1 TeV implies that the possible effects in the $t\bar{t}$ forward-backward asymmetry are less than -0.03% .

Our results should be contrasted with the analysis [21], which finds positive corrections

¹³For a detailed discussion see [52].

¹⁴Including all RS corrections, we find that for the three parameter points considered before, the $t\bar{t}$ forward-backward asymmetry is shifted by -0.04% , -0.05% , and -0.05% with respect to the SM value.

to the $t\bar{t}$ forward-backward asymmetry of up to 5.6% (7%) arising from KK gluons (Z' -boson exchange) at LO. In the latter article, sizable corrections to $C_{q\bar{q}}^A$ arise since the left- and right-handed components of the light-quark fields are localized at different ends of the extra dimension by choosing $c_{u_L} = c_{d_L} \in [-0.4, 0.4]$ (IR-localized) and $c_{u_R} = c_{d_R} = -0.8$ (UV-localized).¹⁵ In an anarchic approach to flavor, such a choice is in conflict with observation, because it fails to reproduce the hierarchies of light-quark masses and mixings.

5 Conclusions and Outlook

In this work we have studied the interplay between new-physics LO and NLO effects to the top-quark forward-backward asymmetry A_{FB}^t within RS models. In scenarios with flavor anarchy, the dominant contributions to $t\bar{t}$ production arise from s -channel exchange of KK gluons. The axial-vector couplings to light quarks are suppressed due to both their UV localization as well as the close separation of wave functions of different chiralities in the extra dimension. The resulting exponential depletion inhibits potentially large s -channel contributions to the asymmetry at tree level. The suppression of flavor-changing $t\bar{u}$ couplings turns out to be even stronger, such that it is impossible to obtain sizable effects in the t channel as well. Consequently, if the quarks are localized in the extra dimension such that their masses and flavor mixings are correctly reproduced, LO corrections to the forward-backward asymmetry in RS models are deemed to be far too small to be able to explain the observed discrepancy between experiment and SM expectation in A_{FB}^t .

We have furthermore shown that vector currents resulting from KK-gluon exchange yield a positive contribution to the asymmetric cross section σ_a at NLO and are not subject to any suppression related to the localization of quark wave functions. Numerically, we found that the ratio of the products of vector and axial-vector couplings of the light quarks and the top quark generically satisfies $(g_V^q g_V^t)/(g_A^q g_A^t) = \mathcal{O}(10^3)$. This strong enhancement implies that, despite their loop suppression, NLO vector-current contributions to the asymmetry exceed the LO axial-vector correction by typically a factor of around 100. However, tree-level vector currents, arising from KK-gluon exchange, tend to also enhance the symmetric cross section $\sigma_s = \sigma_{t\bar{t}}$, which enters the normalization of the $t\bar{t}$ forward-backward asymmetry. Our numerical analysis reveals that in practice the NLO vector contribution to σ_a is cancelled in large parts by the LO contribution to σ_s , so that the resulting sensitivity of $A_{\text{FB}}^t = \sigma_a/\sigma_s$ to vector currents is not very pronounced. This feature not only limits the magnitude of the possible RS contributions in A_{FB}^t to far below the percent level, but also leads to the robust prediction, related to the compositeness of the top quark, that these corrections are necessarily destructive. These findings are largely model-independent, as they do not depend strongly on the exact realization of the electroweak bulk gauge group, the choice of fermion representations, or the precise nature of the Higgs sector of the considered RS setup.

As our arguments are sufficiently general, they do not only apply to the RS framework but to the broader class of models with new heavy vector states that have small axial-vector couplings to light quarks. In particular, many new-physics models which address the flavor

¹⁵Notice that the convention of the bulk mass parameters used in [21] differs from ours by an overall sign.

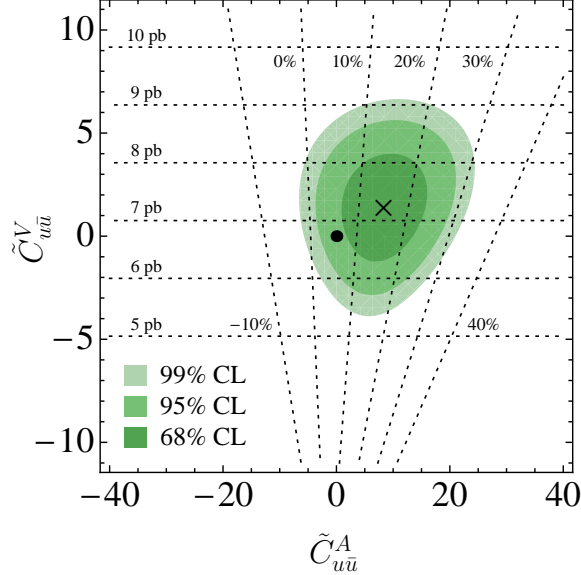


Figure 5: Results of a combined fit to $\sigma_{t\bar{t}}$, the last bin of $d\sigma_{t\bar{t}}/dM_{t\bar{t}}$, and the value of $(A_{\text{FB}}^t)^{p\bar{p}}$ allowing for new physics in s -channel exchange. The green contours indicate, from dark to light, the experimentally favored regions of 68%, 95%, and 99% probability in the $\tilde{C}_{u\bar{u}}^A$ - $\tilde{C}_{u\bar{u}}^V$ plane. The horizontal (almost vertical) dashed lines correspond to the value of the total $t\bar{t}$ cross section (forward-backward asymmetry in the $p\bar{p}$ frame). Further details can be found in the text.

problem via a Froggatt-Nielsen-type mechanism belong to the latter category. The aforementioned cancellation of vector contributions between the numerator and denominator of A_{FB}^t suggests that in such new-physics scenarios, irrespectively of their sign, large contributions to the $t\bar{t}$ forward-backward asymmetry are essentially impossible to achieve, once the experimentally available information on $\sigma_{t\bar{t}}$ and the high-energy tail of the $t\bar{t}$ invariant mass spectrum $d\sigma_{t\bar{t}}/dM_{t\bar{t}}$ is taken into account. This is illustrated in Figure 5, which shows the results of a global fit to the available $t\bar{t}$ data (see (1) and (32)) in the presence of new physics in the s channel. The colored contours indicate the experimentally preferred region in the $\tilde{C}_{u\bar{u}}^A$ - $\tilde{C}_{u\bar{u}}^V$ plane. From the shape and location of the favored area, one infers that a non-zero vector coefficient $\tilde{C}_{u\bar{u}}^V$ alone does not lead to a significant improvement in the quality of the fit, but that large corrections to the axial-vector coefficient $\tilde{C}_{u\bar{u}}^A$ are needed to get from the SM point (black dot) at $(0, 0)$ to the best-fit value (black cross) at $(8.3, 1.4)$. In fact, requiring the three $t\bar{t}$ predictions to be within the global 95% (99%) CL region allows for maximal values $(A_{\text{FB}}^t)^{p\bar{p}}$ of 5.8% (6.0%) from vector contributions alone. The corresponding point in the $\tilde{C}_{u\bar{u}}^A$ - $\tilde{C}_{u\bar{u}}^V$ plane is located at $(0, -1.8)$ ($(0, -3.1)$). We conclude from these general observations that a large $t\bar{t}$ forward-backward asymmetry inevitably has to arise from tree-level effects involving either axial-vector currents in the s channel with flavor-specific couplings of opposite sign to light quarks and top quarks or large flavor-changing currents in the t channel. However, both options are difficult to realize in any explicit construction of physics beyond the SM without invoking additional *ad hoc* assumptions about the flavor structure of the light-quark sector.

There thus seems to be a generic tension between having large effects in A_{FB}^t and achieving a natural solution to the flavor problem.

Acknowledgments

We are grateful to V. Ahrens, A. Ferroglia, M. Neubert, B. Pecjak, and L. Yang for useful discussions. The Feynman diagrams shown in this work are drawn using `FeynArts` [65]. This research is supported in part by the German Federal Ministry for Education and Research grant 05H09UME (“Precision Calculations for Collider and Flavour Physics at the LHC”), the Helmholtz-Institut Mainz, and the Research Centre “Elementary Forces and Mathematical Foundations” funded by the Excellence Initiative of the State of Rhineland-Palatinate. U.H. would like to thank the Aspen Center for Physics, where part of this research was performed.

A Higgs-Boson Phase-Space Factors

In this appendix we present the explicit form of the phase-space factors appearing in the Higgs-boson contribution to the charge-symmetric and -asymmetric part of the $t\bar{t}$ cross section. The functions $f_{S,A}(z)$ introduced in (21) and (22) read

$$\begin{aligned} f_S(z) &= -\frac{\beta\rho}{72} \left[1 + \frac{\rho(1-z)}{2} + \frac{\rho(4+\rho(1-z)^2)}{8\beta} \ln \left(\frac{2(1+\beta) - \rho(1-z)}{2(1-\beta) - \rho(1-z)} \right) \right], \\ f_A(z) &= \frac{\rho}{144} \left[1 - \rho + \frac{\rho(4+\rho(1-z)^2)}{4} \ln \left(\frac{\rho(4z+\rho(1-z)^2)}{(2-\rho(1-z))^2} \right) \right], \end{aligned} \quad (\text{A1})$$

where $z = m_h^2/m_t^2$, $\beta = \sqrt{1-\rho}$, and $\rho = 4m_t^2/\hat{s}$.

B Wilson Coefficients in the ZMA

In the following, we present the ZMA results for the Wilson coefficients in (23). Specializing to the case of the up quark ($q = u$), we find

$$\begin{aligned} C_{u\bar{u},\parallel}^{(V,8)} &= -\frac{4\pi\alpha_s}{M_{\text{KK}}^2} \left[\frac{1}{2L} - \frac{F^2(c_{t_R})(2c_{t_R}+5)}{4(2c_{t_R}+3)^2} - \frac{F^2(c_{t_L})(2c_{t_L}+5)}{4(2c_{t_L}+3)^2} \right. \\ &\quad - \frac{F^2(c_{u_R})}{4|(M_u)_{11}|^2} \sum_{i=1,2,3} \frac{(2c_{u_i}+5)|(M_u)_{1i}|^2}{(2c_{u_i}+3)^2} - \frac{F^2(c_{u_L})}{4|(M_u)_{11}|^2} \sum_{i=1,2,3} \frac{(2c_{Q_i}+5)|(M_u)_{i1}|^2}{(2c_{Q_i}+3)^2} \\ &\quad + \frac{L}{2} \frac{F^2(c_{t_R})F^2(c_{u_R})}{(2c_{t_R}+3)|(M_u)_{11}|^2} \sum_{i=1,2,3} \frac{(c_{u_i}+c_{t_R}+3)|(M_u)_{1i}|^2}{(2c_{u_i}+3)(c_{u_i}+c_{t_R}+2)} \\ &\quad \left. + \frac{L}{2} \frac{F^2(c_{t_L})F^2(c_{u_L})}{(2c_{t_L}+3)|(M_u)_{11}|^2} \sum_{i=1,2,3} \frac{(c_{Q_i}+c_{t_L}+3)|(M_u)_{i1}|^2}{(2c_{Q_i}+3)(c_{Q_i}+c_{t_L}+2)} \right], \end{aligned}$$

$$\begin{aligned}
C_{u\bar{u},\perp}^{(V,8)} = & -\frac{4\pi\alpha_s}{M_{\text{KK}}^2} \left[\frac{1}{2L} - \frac{F^2(c_{t_R})(2c_{t_R}+5)}{4(2c_{t_R}+3)^2} - \frac{F^2(c_{t_L})(2c_{t_L}+5)}{4(2c_{t_L}+3)^2} \right. \\
& - \frac{F^2(c_{u_R})}{4|(M_u)_{11}|^2} \sum_{i=1,2,3} \frac{(2c_{u_i}+5)|(M_u)_{1i}|^2}{(2c_{u_i}+3)^2} - \frac{F^2(c_{u_L})}{4|(M_u)_{11}|^2} \sum_{i=1,2,3} \frac{(2c_{Q_i}+5)|(M_u)_{i1}|^2}{(2c_{Q_i}+3)^2} \\
& + \frac{L}{2} \frac{F^2(c_{t_L})F^2(c_{u_R})}{(2c_{t_L}+3)|(M_u)_{11}|^2} \sum_{i=1,2,3} \frac{(c_{u_i}+c_{t_L}+3)|(M_u)_{1i}|^2}{(2c_{u_i}+3)(c_{u_i}+c_{t_L}+2)} \\
& \left. + \frac{L}{2} \frac{F^2(c_{t_R})F^2(c_{u_L})}{(2c_{t_R}+3)|(M_u)_{11}|^2} \sum_{i=1,2,3} \frac{(c_{Q_i}+c_{t_R}+3)|(M_u)_{i1}|^2}{(2c_{Q_i}+3)(c_{Q_i}+c_{t_R}+2)} \right], \tag{B1}
\end{aligned}$$

and similar relations hold in the case of the remaining light quarks $q = d, s, c$. Here $(M_u)_{ij}$ are the minors of the up-type Yukawa matrix Y_u . For the t -channel Wilson coefficients in the vector channel, we obtain

$$\begin{aligned}
C_{t\bar{u},\parallel}^{(V,8)} = & -\frac{\pi\alpha_s}{M_{\text{KK}}^2} L \left[\frac{F^2(c_{t_R})F^2(c_{u_R})|(M_u)_{13}|^2}{(2c_{t_R}+3)(c_{t_R}+1)|(M_u)_{11}|^2} + \frac{F^2(c_{t_L})F^2(c_{u_L})|(M_u)_{31}|^2}{(2c_{t_L}+3)(c_{t_L}+1)|(M_u)_{11}|^2} \right], \\
C_{t\bar{u},\parallel}^{(V,1)} = & -\frac{\pi\alpha_e}{M_{\text{KK}}^2} \frac{L}{s_w^2 c_w^2} \left[(T_3^u - Q_u s_w^2)^2 \frac{F^2(c_{t_L})F^2(c_{u_L})|(M_u)_{31}|^2}{(2c_{t_L}+3)(c_{t_L}+1)|(M_u)_{11}|^2} \right. \\
& \left. + (s_w^2 Q_u)^2 \frac{F^2(c_{t_R})F^2(c_{u_R})|(M_u)_{13}|^2}{(2c_{t_R}+3)(c_{t_R}+1)|(M_u)_{11}|^2} \right] \\
& - \frac{\pi\alpha_e Q_u^2}{M_{\text{KK}}^2} L \left[\frac{F^2(c_{t_R})F^2(c_{u_R})|(M_u)_{13}|^2}{(2c_{t_R}+3)(c_{t_R}+1)|(M_u)_{11}|^2} + \frac{F^2(c_{t_L})F^2(c_{u_L})|(M_u)_{31}|^2}{(2c_{t_L}+3)(c_{t_L}+1)|(M_u)_{11}|^2} \right]. \tag{B2}
\end{aligned}$$

For completeness we also give the result of the Higgs-boson contribution to the t channel. We find for the dimensionless coefficient

$$\tilde{C}_{t\bar{u}}^S = |(g_h^u)_{13}|^2 + |(g_h^u)_{31}|^2, \tag{B3}$$

where

$$\begin{aligned}
(g_h^u)_{13} = & -\frac{m_u}{v} \frac{m_t^2}{M_{\text{KK}}^2} \left(W_u^\dagger \text{diag} \left[\frac{1}{1-2c_{u_i}} \left(\frac{1}{F^2(c_{u_i})} - 1 + \frac{F^2(c_{u_i})}{3+2c_{u_i}} \right) \right] W_u \right)_{13} \\
& + \frac{v^2}{3\sqrt{2}M_{\text{KK}}^2} \left(U_u^\dagger \text{diag} [F(c_{Q_i})] Y_u Y_u^\dagger Y_u \text{diag} [F(c_{u_i})] W_u \right)_{13}, \\
(g_h^u)_{31} = & -\frac{m_u}{v} \frac{m_t^2}{M_{\text{KK}}^2} \left(U_u^\dagger \text{diag} \left[\frac{1}{1-2c_{Q_i}} \left(\frac{1}{F^2(c_{Q_i})} - 1 + \frac{F^2(c_{Q_i})}{3+2c_{Q_i}} \right) \right] U_u \right)_{31} \\
& + \frac{v^2}{3\sqrt{2}M_{\text{KK}}^2} \left(U_u^\dagger \text{diag} [F(c_{Q_i})] Y_u Y_u^\dagger Y_u \text{diag} [F(c_{u_i})] W_u \right)_{31}, \tag{B4}
\end{aligned}$$

and the 3×3 unitary matrices U_u and W_u are defined through

$$\text{diag}[F(c_{Q_i})] Y_u \text{diag}[F(c_{u_i})] = \frac{\sqrt{2}}{v} U_u \text{diag}[m_u, m_c, m_t] W_u^\dagger. \quad (\text{B5})$$

C RG Evolution of the Wilson Coefficients

This appendix contains analytic formulas relating the Wilson coefficients evaluated at the top-quark mass scale m_t with their initial conditions calculated at $M_{\text{KK}} \gg m_t$. Since in the RS model the t -channel Wilson coefficients $\tilde{C}_{t\bar{u}}^V$ and $\tilde{C}_{t\bar{u}}^S$ turn out to be numerically irrelevant, we will not consider their running in the following. We perform the RG evolution at leading-logarithmic accuracy, *i.e.*, at one-loop order, neglecting tiny effects that arise from the mixing with QCD penguin operators. For the s -channel Wilson coefficients entering the formulas (33) and (37), we find for $P = V, A$,

$$\tilde{C}_{q\bar{q}}^P(m_t) = \left(\frac{2}{3\eta^{4/7}} + \frac{\eta^{2/7}}{3} \right) \tilde{C}_{q\bar{q}}^P(M_{\text{KK}}), \quad (\text{C1})$$

where $\eta \equiv \alpha_s(M_{\text{KK}})/\alpha_s(m_t)$ is the ratio of strong coupling constants evaluated at the relevant scales M_{KK} and m_t .

In order to get an idea of the potential impact of RG effects, we evaluate (C1) using $\alpha_s(M_Z) = 0.139$, $M_{\text{KK}} = 1$ TeV, and $m_t = 173.1$ GeV, which leads to $\eta = 0.803$ at one-loop order. We obtain

$$\tilde{C}_{q\bar{q}}^P(m_t) = 1.07 \tilde{C}_{q\bar{q}}^P(M_{\text{KK}}), \quad (\text{C2})$$

from which we conclude that the RG evolution increases the Wilson coefficients $\tilde{C}_{q\bar{q}}^P$ by about 7% with respect to the values quoted in Table 1. Operator mixing thus represents only a numerically subdominant effect.

D Parameter Points

In order to make our work self-contained, we specify in this appendix the complete set of model parameters, namely the bulk mass parameters of the quark fields and the Yukawa matrices, corresponding to the three parameter points used in our numerical analysis. All the parameter sets given below have been obtained by random choice, subject to the constraints that the absolute value of each entry in $Y_{u,d}$ is between 1/3 and 3, and that the Wolfenstein parameters $\bar{\rho}$ and $\bar{\eta}$ agree with experiment within errors. The bulk mass parameters have then been determined using the warped-space Froggatt-Nielsen formulas given in [49], which guarantees that the quark masses and mixings are correctly reproduced. For further details concerning the algorithm used to scan the parameter space of the RS model, the interested reader is referred to [48].

Our first parameter point is specified by the following bulk mass parameters¹⁶

$$\begin{aligned}
c_{Q_1} &= -0.611, & c_{Q_2} &= -0.580, & c_{Q_3} &= -0.407, \\
c_{u_1} &= -0.688, & c_{u_2} &= -0.550, & c_{u_3} &= +0.091, \\
c_{d_1} &= -0.665, & c_{d_2} &= -0.627, & c_{d_3} &= -0.577,
\end{aligned} \tag{D1}$$

and Yukawa matrices

$$\begin{aligned}
\mathbf{Y}_u &= \begin{pmatrix} -1.303 - 0.364i & -1.215 + 0.089i & -1.121 - 1.679i \\ 1.857 + 1.199i & 2.038 + 1.105i & -0.484 - 0.193i \\ -1.052 + 0.546i & -2.833 + 0.191i & -1.287 - 1.141i \end{pmatrix}, \\
\mathbf{Y}_d &= \begin{pmatrix} -0.661 - 1.118i & -0.075 - 0.656i & 0.141 - 0.465i \\ -2.070 + 1.364i & -2.518 + 1.435i & 0.717 - 0.165i \\ 0.306 + 2.830i & 0.034 - 0.350i & -0.951 - 0.829i \end{pmatrix}.
\end{aligned} \tag{D2}$$

The second parameter point is given by

$$\begin{aligned}
c_{Q_1} &= -0.646, & c_{Q_2} &= -0.573, & c_{Q_3} &= -0.449, \\
c_{u_1} &= -0.658, & c_{u_2} &= -0.513, & c_{u_3} &= +0.480, \\
c_{d_1} &= -0.645, & c_{d_2} &= -0.626, & c_{d_3} &= -0.578,
\end{aligned} \tag{D3}$$

and

$$\begin{aligned}
\mathbf{Y}_u &= \begin{pmatrix} 0.637 - 1.800i & 1.518 - 2.209i & 0.904 + 0.146i \\ 0.219 - 0.207i & -0.333 - 0.942i & 0.597 + 0.020i \\ 1.829 + 1.538i & -0.018 + 1.772i & -1.258 + 1.265i \end{pmatrix}, \\
\mathbf{Y}_d &= \begin{pmatrix} -2.835 - 0.946i & -0.404 + 0.746i & -1.135 + 0.060i \\ 0.724 - 0.350i & -2.214 - 0.555i & 0.610 - 0.051i \\ 0.701 - 0.101i & -0.154 + 0.104i & 1.514 + 0.919i \end{pmatrix}.
\end{aligned} \tag{D4}$$

Finally, our third parameter point features

$$\begin{aligned}
c_{Q_1} &= -0.624, & c_{Q_2} &= -0.563, & c_{Q_3} &= -0.468, \\
c_{u_1} &= -0.712, & c_{u_2} &= -0.560, & c_{u_3} &= +0.899, \\
c_{d_1} &= -0.659, & c_{d_2} &= -0.642, & c_{d_3} &= -0.571,
\end{aligned} \tag{D5}$$

¹⁶Here and below, results are given to at least three significant digits.

and

$$\begin{aligned}
\mathbf{Y}_u &= \begin{pmatrix} -0.541 + 1.517i & -1.083 + 1.857i & 1.718 - 2.057i \\ 0.359 - 1.713i & -2.208 + 1.404i & -1.160 + 0.886i \\ -1.172 - 0.543i & -0.116 - 0.238i & -0.669 - 1.688i \end{pmatrix}, \\
\mathbf{Y}_d &= \begin{pmatrix} -0.878 - 1.677i & 0.190 + 0.573i & -0.817 + 2.663i \\ -1.792 + 0.861i & -2.880 + 0.132i & -0.070 - 1.151i \\ -1.679 + 1.588i & 0.972 + 0.615i & 1.421 + 0.981i \end{pmatrix}.
\end{aligned}
\tag{D6}$$

Here $c_{Q_1} = c_{u_L} = c_{d_L}$, $c_{u_1} = c_{u_R}$, and $c_{d_1} = c_{d_R}$ and similarly in the case of the second and third quark generation.

References

- [1] The Tevatron Electroweak Working Group for the CDF and DØ Collaborations, arXiv:0903.2503 [hep-ex].
- [2] E. Thomson *et al.* [CDF Collaboration], Conference Note 9913, October 19, 2009, http://www-cdf.fnal.gov/physics/new/top/2009/xsection/ttbar_combined_46invfb/
- [3] DØ Collaboration, Conference Note 5907-CONF, March 12, 2009, <http://www-d0.fnal.gov/Run2Physics/WWW/results/prelim/TOP/T79/>
- [4] T. Aaltonen *et al.* [CDF Collaboration], Phys. Rev. Lett. **100**, 231801 (2008) [arXiv:0709.0705 [hep-ex]].
- [5] T. Aaltonen *et al.* [CDF Collaboration], Phys. Rev. D **77**, 051102 (2008) [arXiv:0710.5335 [hep-ex]].
- [6] V. M. Abazov *et al.* [DØ Collaboration], Phys. Lett. B **668**, 98 (2008) [arXiv:0804.3664 [hep-ex]].
- [7] A. Bridgeman, FERMILAB-THESIS-2008-50.
- [8] T. Aaltonen *et al.* [CDF Collaboration], Phys. Rev. Lett. **102**, 222003 (2009) [arXiv:0903.2850 [hep-ex]].
- [9] T. A. Schwarz, FERMILAB-THESIS-2006-51, UMI-32-38081.
- [10] V. M. Abazov *et al.* [DØ Collaboration], Phys. Rev. Lett. **100**, 142002 (2008) [arXiv:0712.0851 [hep-ex]].
- [11] T. Aaltonen *et al.* [CDF Collaboration], Phys. Rev. Lett. **101**, 202001 (2008) [arXiv:0806.2472 [hep-ex]].

- [12] G. Strycker *et al.* [CDF Collaboration], CDF/ANAL/TOP/PUBLIC/9724 Note, March 17, 2009, <http://www-cdf.fnal.gov/physics/new/top/2009/tprop/Afb/>
- [13] G. Strycker *et al.* [CDF Collaboration], CDF/ANAL/TOP/PUBLIC/10224 Note, July 14, 2010, <http://www-cdf.fnal.gov/physics/new/top/2010/tprop/Afb/>
- [14] DØ Collaboration, Conference Note 6062-CONF, July 23, 2010, <http://www-d0.fnal.gov/Run2Physics/WWW/results/prelim/TOP/T90/>
- [15] J. H. Kühn and G. Rodrigo, Phys. Rev. Lett. **81**, 49 (1998) [arXiv:hep-ph/9802268].
- [16] J. H. Kühn and G. Rodrigo, Phys. Rev. D **59**, 054017 (1999) [arXiv:hep-ph/9807420].
- [17] O. Antunano, J. H. Kühn, and G. Rodrigo, Phys. Rev. D **77**, 014003 (2008), [arXiv:0709.1652 [hep-ph]].
- [18] L. G. Almeida, G. Stermann and W. Vogelsang, Phys. Rev. D **78**, 014008 (2008) [arXiv:0805.1885 [hep-ph]].
- [19] V. Ahrens, A. Ferroglia, M. Neubert, B. D. Pecjak and L. L. Yang, JHEP **1009**, 097 (2010) [arXiv:1003.5827 [hep-ph]].
- [20] K. Melnikov and M. Schulze, Nucl. Phys. B **840**, 129 (2010) [arXiv:1004.3284 [hep-ph]].
- [21] A. Djouadi, G. Moreau, F. Richard and R. K. Singh, Phys. Rev. D **82**, 071702 (2010) [arXiv:0906.0604 [hep-ph]].
- [22] P. Ferrario and G. Rodrigo, Phys. Rev. D **80**, 051701 (2009) [arXiv:0906.5541 [hep-ph]].
- [23] S. Jung, H. Murayama, A. Pierce and J. D. Wells, Phys. Rev. D **81**, 015004 (2010) [arXiv:0907.4112 [hep-ph]].
- [24] K. Cheung, W. Y. Keung and T. C. Yuan, Phys. Lett. B **682**, 287 (2009) [arXiv:0908.2589 [hep-ph]].
- [25] P. H. Frampton, J. Shu and K. Wang, Phys. Lett. B **683**, 294 (2010) [arXiv:0911.2955 [hep-ph]].
- [26] J. Shu, T. M. P. Tait and K. Wang, Phys. Rev. D **81**, 034012 (2010) [arXiv:0911.3237 [hep-ph]].
- [27] A. Arhrib, R. Benbrik and C. H. Chen, Phys. Rev. D **82**, 034034 (2010) [arXiv:0911.4875 [hep-ph]].
- [28] I. Dorsner, S. Fajfer, J. F. Kamenik and N. Kosnik, Phys. Rev. D **81**, 055009 (2010) [arXiv:0912.0972 [hep-ph]].
- [29] D. W. Jung, P. Ko, J. S. Lee and S. h. Nam, Phys. Lett. B **691**, 238 (2010) [arXiv:0912.1105 [hep-ph]].

- [30] J. Cao, Z. Heng, L. Wu and J. M. Yang, Phys. Rev. D **81**, 014016 (2010) [arXiv:0912.1447 [hep-ph]].
- [31] V. Barger, W. Y. Keung and C. T. Yu, Phys. Rev. D **81**, 113009 (2010) [arXiv:1002.1048 [hep-ph]].
- [32] Q. H. Cao, D. McKeen, J. L. Rosner, G. Shaughnessy and C. E. M. Wagner, Phys. Rev. D **81**, 114004 (2010) [arXiv:1003.3461 [hep-ph]].
- [33] B. Xiao, Y. k. Wang and S. h. Zhu, Phys. Rev. D **82**, 034026 (2010) [arXiv:1006.2510 [hep-ph]].
- [34] R. S. Chivukula, E. H. Simmons and C. P. Yuan, arXiv:1007.0260 [hep-ph].
- [35] P. Ferrario and G. Rodrigo, Phys. Rev. D **78**, 094018 (2008) [arXiv:0809.3354 [hep-ph]].
- [36] P. Ferrario and G. Rodrigo, JHEP **1002**, 051 (2010) [arXiv:0912.0687 [hep-ph]].
- [37] C. D. Froggatt and H. B. Nielsen, Nucl. Phys. B **147**, 277 (1979).
- [38] L. Randall and R. Sundrum, Phys. Rev. Lett. **83**, 3370 (1999) [arXiv:hep-ph/9905221].
- [39] N. Arkani-Hamed and M. Schmaltz, Phys. Rev. D **61**, 033005 (2000) [arXiv:hep-ph/9903417].
- [40] H. Davoudiasl, J. L. Hewett and T. G. Rizzo, Phys. Lett. B **473**, 43 (2000) [arXiv:hep-ph/9911262].
- [41] A. Pomarol, Phys. Lett. B **486**, 153 (2000) [arXiv:hep-ph/9911294].
- [42] Y. Grossman and M. Neubert, Phys. Lett. B **474**, 361 (2000) [arXiv:hep-ph/9912408].
- [43] S. Chang, J. Hisano, H. Nakano, N. Okada and M. Yamaguchi, Phys. Rev. D **62**, 084025 (2000) [arXiv:hep-ph/9912498].
- [44] T. Gherghetta and A. Pomarol, Nucl. Phys. B **586**, 141 (2000) [arXiv:hep-ph/0003129].
- [45] S. J. Huber and Q. Shafi, Phys. Lett. B **498**, 256 (2001) [arXiv:hep-ph/0010195].
- [46] S. J. Huber, Nucl. Phys. B **666**, 269 (2003) [arXiv:hep-ph/0303183].
- [47] K. Agashe, G. Perez and A. Soni, Phys. Rev. D **71**, 016002 (2005) [arXiv:hep-ph/0408134].
- [48] M. Bauer, S. Casagrande, U. Haisch and M. Neubert, JHEP **1009**, 017 (2010) [arXiv:0912.1625 [hep-ph]].
- [49] S. Casagrande, F. Goertz, U. Haisch, M. Neubert and T. Pfoh, JHEP **0810**, 094 (2008) [arXiv:0807.4937 [hep-ph]].

- [50] M. Blanke, A. J. Buras, B. Duling, S. Gori and A. Weiler, *JHEP* **0903**, 001 (2009) [arXiv:0809.1073 [hep-ph]].
- [51] M. Bauer, S. Casagrande, L. Gründer, U. Haisch and M. Neubert, *Phys. Rev. D* **79**, 076001 (2009) arXiv:0811.3678 [hep-ph].
- [52] S. Casagrande, F. Goertz, U. Haisch, M. Neubert and T. Pfoh, *JHEP* **1009**, 014 (2010) [arXiv:1005.4315 [hep-ph]].
- [53] K. Agashe, A. Belyaev, T. Krupovnickas, G. Perez and J. Virzi, *Phys. Rev. D* **77**, 015003 (2008) [arXiv:hep-ph/0612015].
- [54] F. A. Berends, K. J. F. Gaemers and R. Gastmans, *Nucl. Phys. B* **63**, 381 (1973).
- [55] F. A. Berends, R. Kleiss, S. Jadach and Z. Was, *Acta Phys. Polon. B* **14**, 413 (1983).
- [56] T. Hahn, *Comput. Phys. Commun.* **168**, 78 (2005) [arXiv:hep-ph/0404043].
- [57] A. D. Martin, W. J. Stirling, R. S. Thorne and G. Watt, *Eur. Phys. J. C* **63**, 189 (2009) [arXiv:0901.0002 [hep-ph]].
- [58] P. Nason, S. Dawson and R. K. Ellis, *Nucl. Phys. B* **303**, 607 (1988).
- [59] J. Campbell and R. K. Ellis, <http://mcfm.fnal.gov>
- [60] M. Cacciari, S. Frixione, M. L. Mangano, P. Nason and G. Ridolfi, *JHEP* **0809**, 127 (2008) [arXiv:0804.2800 [hep-ph]].
- [61] N. Kidonakis and R. Vogt, *Phys. Rev. D* **78**, 074005 (2008) [arXiv:0805.3844 [hep-ph]].
- [62] U. Langenfeld, S. Moch and P. Uwer, *Phys. Rev. D* **80**, 054009 (2009) [arXiv:0906.5273 [hep-ph]].
- [63] V. Ahrens, A. Ferroglia, M. Neubert, B. D. Pecjak and L. L. Yang, *Phys. Lett. B* **687**, 331 (2010) [arXiv:0912.3375 [hep-ph]].
- [64] W. Bernreuther and Z. G. Si, *Nucl. Phys. B* **837**, 90 (2010) [arXiv:1003.3926 [hep-ph]].
- [65] T. Hahn, *Comput. Phys. Commun.* **140**, 418 (2001) [arXiv:hep-ph/0012260].